RELATIONSHIPS BETWEEN THE SULPHIDE MINERALS, METAMORPHISM, AND DEFORMATION IN THE FARIBAULT BROOK AREA OF THE CAPE BRETON HIGHLANDS, NOVA SCOTIA

by

KAREN CONNORS

Submitted in partial fulfillment of the requirements for a Bachelor of Science (Honours) Degree

Dalhousie University
Halifax, Nova Scotia
March, 1986

DALHOUSIE UNIVERSITY
Department of Geology
Halifax, N.S. Canada B3H 3J5 Telephone (902) 424-2358 Telex: 019-21863

DALHOUSIE UNIVERSITY, DEPARTMENT OF GEOLOGY

B.Sc. HONOURS THESIS

Author: Karen A. Connors

Title: Relationships between the sulphide minerals, metamorphism, and deformation in the Faribault Brook area of the Cape Breton Highlands, Nova Scotia

Date: April 1/1986

Distribution License

DalSpace requires agreement to this non-exclusive distribution license before your item can appear on DalSpace.

NON-EXCLUSIVE DISTRIBUTION LICENSE

You (the author(s) or copyright owner) grant to Dalhousie University the non-exclusive right to reproduce and distribute your submission worldwide in any medium.

You agree that Dalhousie University may, without changing the content, reformat the submission for the purpose of preservation.

You also agree that Dalhousie University may keep more than one copy of this submission for purposes of security, back-up and preservation.

You agree that the submission is your original work, and that you have the right to grant the rights contained in this license. You also agree that your submission does not, to the best of your knowledge, infringe upon anyone's copyright.

If the submission contains material for which you do not hold copyright, you agree that you have obtained the unrestricted permission of the copyright owner to grant Dalhousie University the rights required by this license, and that such third-party owned material is clearly identified and acknowledged within the text or content of the submission.

If the submission is based upon work that has been sponsored or supported by an agency or organization other than Dalhousie University, you assert that you have fulfilled any right of review or other obligations required by such contract or agreement.

Dalhousie University will clearly identify your name(s) as the author(s) or owner(s) of the submission, and will not make any alteration to the content of the files that you have submitted.

If you have questions regarding this license please contact the repository manager at dalspace@dal.ca.

Grant the distribution license by signing and dating below.

Name of signatory	Date

TABLE OF CONTENTS

1.	INTRODUCTION	1
	1.1 GENERAL	1
	1.2 PHYSIOGRAPHY AND GEOGRAPHY	3
	1.3 REGIONAL GEOLOGY	6
	1.4 PREVIOUS WORK	8
	1.5 OBJECTIVES AND APPROACH	8
2.	LITHOLOGIES AND FIELD RELATIONS	11
	2.1 INTRODUCTION	11
	2.2 METAVOLCANIC UNIT	13
	2.3 METASEDIMENTARY UNIT	18
	2.4 INTRUSIVE UNITS	20
	2.5 DISCUSSION	21
3.	STRUCTURE	23
	3.1 INTRODUCTION	23
	3.2 ISOCLINAL FOLDING	23
	3.3 FOLIATION	25
	3.4 DUCTILE SHEARING	29
	3.5 UPRIGHT FOLDING	30
	3.6 CRENULATIONS AND LINEATIONS	33
	3.7 KINKING	33
	3.8 FALUTING	34
	3.9 BRITTLE SHEARING	36
	3.10 DISCUSSION	36
4.	METAMORPHISM	39
	4.1 INTRODUCTION	39
	4.2 METAMORPHIC ASSEMBLAGES AND TEXTURES	39
	4.2.1 METAVOLCANIC UNIT	40
	4.2.2 METASEDIMENTARY UNIT	44
	4.2.3 INTRUSIVE UNITS	48
	4.3 DISCUSSION	51
5.	GEOCHEMISTRY	56
	5.1 INTRODUCTION	56
	5.2 GENERAL CHEMISTRY	56
	5.3 DISCRIMINANT DIAGRAMS	57
	5.4 COMPARISONS	66
	5.5 DISCUSSION	68

6. ECONOMIC GEOLOGY 71

6.1 INTRODUCTION 71
6.2 MINOR OCCURRENCES 72
6.3 GALENA MINE 74
6.4 CORE SHACK 75
6.5 SILVER CLIFF 76
6.6 MINERALIZED SHEAR ZONES 79
6.7 DISCUSSION 80

7. DISCUSSION AND CONCLUSIONS 84

8. IMPLICATIONS AND RECOMMENDATIONS 88

REFERENCES 90

LIST OF FIGURES

1.1	MAP OF REGIONAL GEOLOGY	2
1.2	MAP OF STUDY AREA	4
2.1	LITHOLOGIC SECTION	12
2.2	PILLOW BASALTS	15
2.3	CARBONATE CAVITIES	16
2.4	RADIAL FRACTURES	16
3.1	BEDDING PARALLEL FOLIATION	26
3.2	FOLIATION IN A HINGE ZONE	27
3.3	FOLIATION IN PSAMMITES	28
3.4	CONTOURED STEREOGRAM OF FOLIATIONS	31
3.5	CONTOURED STEREOGRAM OF LINEATIONS AND CRENULATION AXES	32
4.1	PRIMARY TEXTURES IN QUARTZ	42
4.2	GARNET SURROUNDING SULPHIDES	43
4.3	INCLUSION TRAILS IN GARNET	45
4.4	GARNET GROWTH DURING FLATTENING	49
4.5	INTERGROWTH OF HORNBLENDE AND SULPHIDES	50
4.6	PETROGENETIC GRID	53
4.7	SUMMARY TABLE	54
5.1	PLOT OF TiO_2-P_2O_5-K_2O	59
5.2	PLOT OF TiO_2 VS Zr	60
5.3	PLOT OF DISCRIMINANT FUNCTIONS	61
5.4	PLOT OF TiO_2-P_2O_5-MnO	62
5.5	PLOT OF Ti-Zr-Y	63

5.6 PLOT OF Ti VS Zr 64

5.7 PLOT OF Ti-Zr-Sr 65

6.1 PARALLEL OXIDES IN PELITES 73

6.2 SULPHIDES PARALLEL TO THE FOLIATION 73

6.3 FOLDING AND SHEARING IN A SULPHIDE LAYER 77

6.4 BRITTLE DEFORMATION OF SULPHIDES 78

6.5 GALENA WITHIN THE FOLIATION PLANE 78

6.6 MnO OXIDE OR HYDROXIDE 81

6.7 HEMATITE REPLACING PYRRHOTITE 81

A.1 SAMPLE LOCATION MAP 101

ABSTRACT

The study area is located within the Jumping Brook Complex which is part of the western Highlands volcanic sedimentary complex. In the Faribault Brook area, the Jumping Brook Complex consists of a unit of pillow basalts which is overlain by a sedimentary sequence with interbedded felsic volcanic layers near the base. The units have undergone upper greenschist to lower amphibolite facies metamorphism and polyphase deformation. The main fabric consists of a pervasive foliation and a later crenulation which locally dominates in the finer grained metasedimentary layers. Prograde metamorphism peaked late in the deformation, during or after the development of the crenulation.

Sulphide minerals are found throughout both the metavolcanic and metasedimentary units, but the main concentrations of base metal sulphides are associated with the felsic volcanic layers. The presence of the sulphide minerals prior to metamorphism and deformation is indicated by alignment parallel to the foliation and crenulation, metamorphic recrystallization, and brittle deformation of these minerals. Significant concentrations of sulphides are also associated with ductile shear zones, thus indicating that remobilization of the sulphide minerals has occurred. The presence of the sulphides prior to deformation and the

association with the felsic volcanic layers suggests that the base metal deposits are syngenetic.

Discriminant diagrams of the geochemical data indicate that the pillow basalts may have formed in an island arc environment. The sequence of lithologies and field evidence support this type of environment. The presence of a syngenetic base metal deposit in an island arc sequence suggests that the sulphides may have formed as a volcanogenic exhalative deposit.

ACKNOWLEDGEMENTS

My sincere thanks go to R.A. Jamieson and M. Zentilli for guidance and many discussions throughout the course of this project; to G. Brown and K. Maxwell for thin and polished section preparation; to K. Cameron of Saint Mary's University for geochemical analyses; and to H. Plint for her assistance during the field work for this project and advice throughout its progress. Special thanks go to G. Woods of Selco for permission to work on the company's claims.

CHAPTER ONE

INTRODUCTION

1.1 GENERAL

The western Highlands volcanic sedimentary complex (Barr _et al_., 1985), which includes the Jumping Brook Complex (Currie, 1982, in press), is a north-south trending belt located in the western Cape Breton Highlands (figure 1.1). Numerous polymetallic (Cu, Zn, Pb, Au, Ag) mineral occurrences are associated with the metavolcanic sequences (eg. Ponsford and Lyttle, 1984, Chatterjee, 1980, and Milligan, 1970). Many showings have been explored and limited mining was conducted in the early 1900's, but no significant deposits have been located. This may, in part, be due to a lack of understanding of the geological setting and history (stratigraphic, structural, metamorphic, and plutonic) of the occurrences (Plint _et al_., in prep). Renewed interest in exploration points to the need for a better understanding and recent work (eg. Barr _et al_., 1985, Craw, 1984, Raeside _et al_., 1984, Jamieson and Craw, 1983, Jamieson and Doucet, 1983) has contributed towards a detailed geological base map which can be used as a framework in which to place the mineral occurrences.

This study was undertaken to examine in detail the stratigraphic, structural, and metamorphic relationships

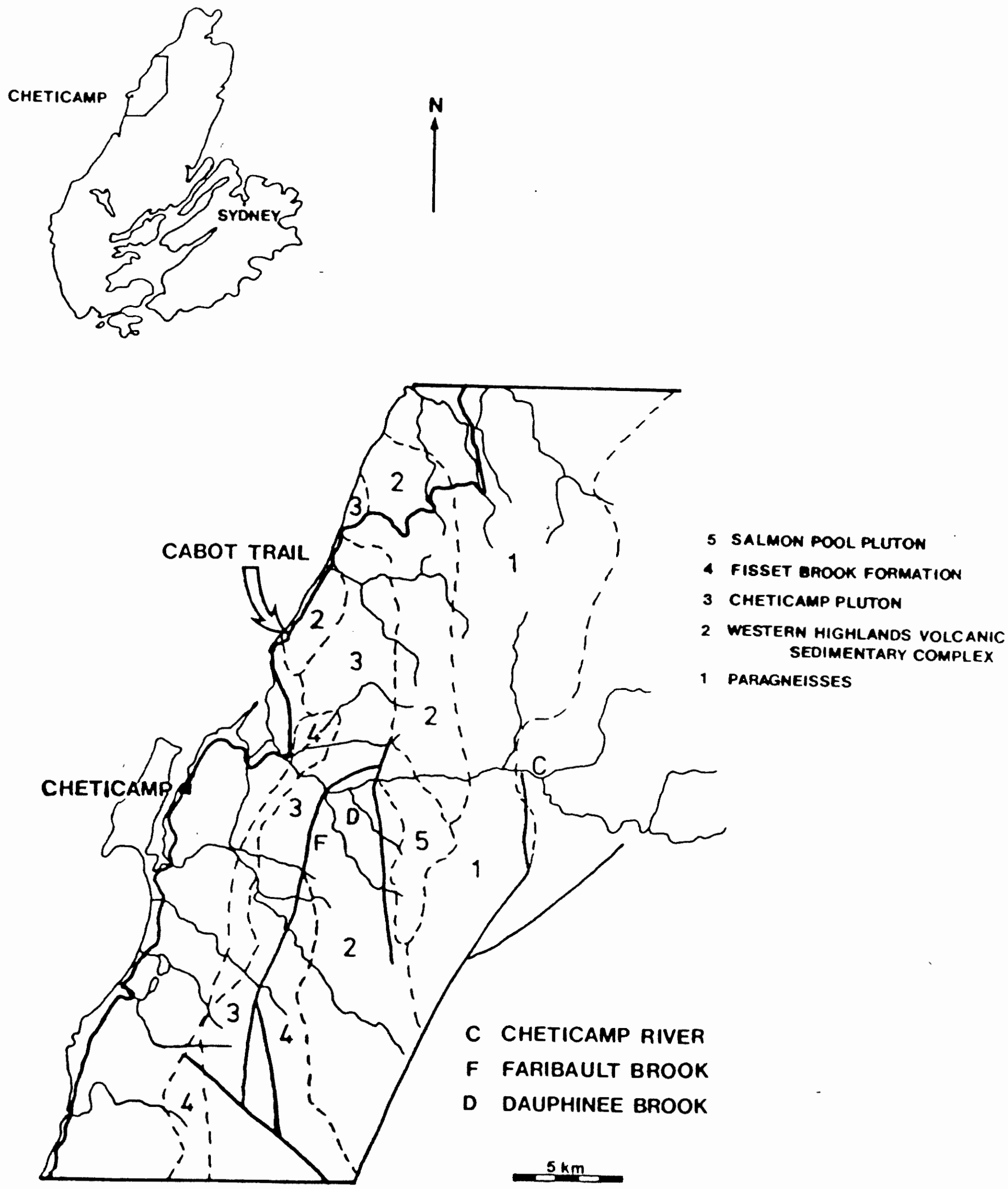

Figure 1.1 Map of the regional geology showing the units which are located adjacent to the western Highlands volcanic sedimentary complex. The unlabelled section along the coast consists of Carboniferous sediments. Inset shows the location of the map. Heavy lines denote faults (after Jamieson and Craw, 1983).

between the sulphide mineralization and the metavolcanic - metasedimentary host in the vicinity of Faribault and Dauphinee Brooks (figure 1.1).

1.2 PHYSIOGRAPHY AND GEOGRAPHY

The study area (figure 1.2) is approximately two square kilometres in size and is located at the intersection of map sheets 11K/10-U1,U2,U3,U4 of the Topographic (orthophoto) Map series for Nova Scotia. Faribault Brook lies 5-6 km inland from the west coast and access is obtained via an old mining road known as the Acadian Trail (figure 1.2), which intersects the Cabot Trail just north of Cheticamp.

The area is densely wooded with a mixture of deciduous and coniferous trees which is typical for the Cape Breton Highlands. Thus, outcrop is largely restricted to the rivers and brooks. Populated areas in this region are confined to the Carboniferous plain along the coast and generally border the Cabot Trail.

The topography is marked by steep river valleys and broad flat hills. Relief in the study area ranges from 50 metres above sea level where Faribault Brook runs into the Cheticamp River to almost 400 metres above sea level at the crest of the ridge which lies between Faribault and Dauphinee Brooks. Drainage is chiefly to the north where the brooks run into the Cheticamp River, which in turn flows

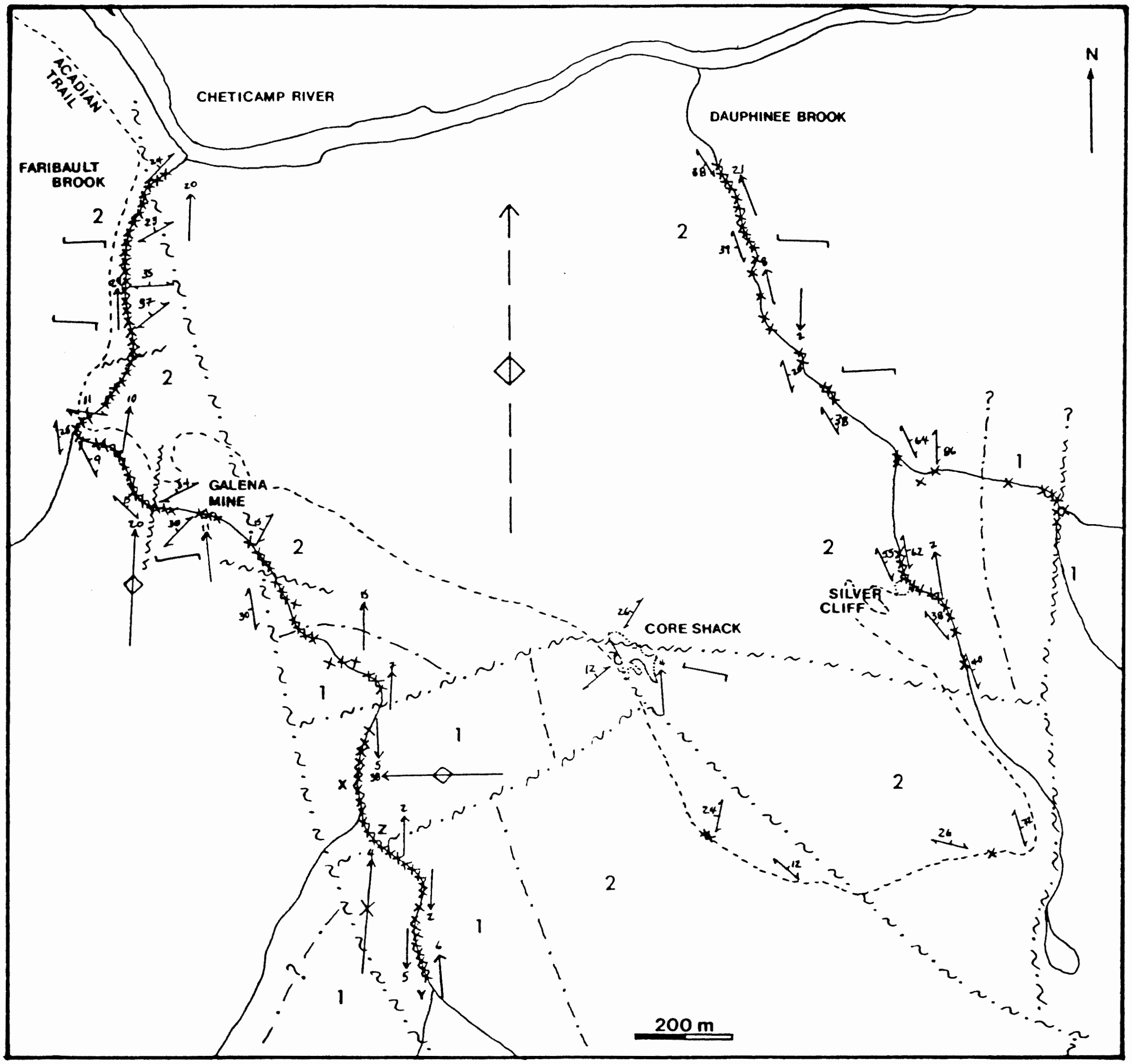

Figure 1.2 Map of the study area. Contacts between the metasedimentary and metavolcanic units are modified after Covey (1979). The legend is given on the following page.

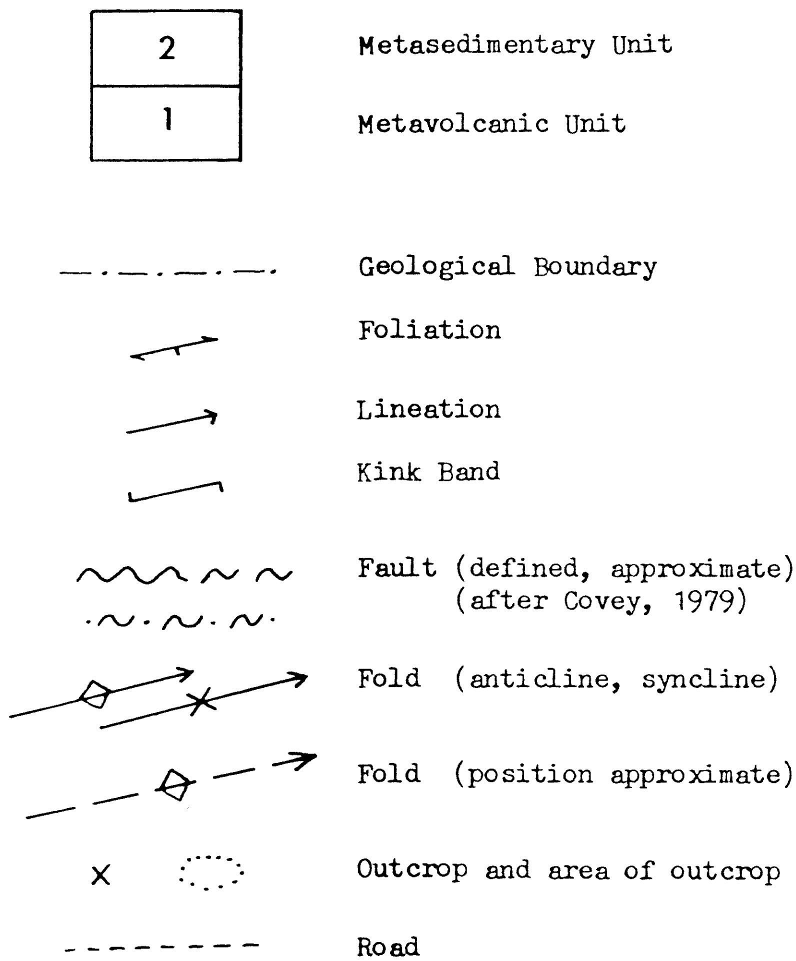

Figure 1.2 Legend for the field map.

westward into the Gulf of St. Lawrence.

1.3 REGIONAL GEOLOGY

The central northwest area of Cape Breton Island, known as the Cape Breton Highlands, consists of a complex assortment of variably metamorphosed volcanic, sedimentary, and plutonic units (eg. Barr et al., 1985 and Plint et al., in prep). In the Cheticamp River area, the Jumping Brook Complex is adjacent to a unit of paragneisses to the east (figure 1.1). The paragneisses are considered to be the high grade equivalent of the low grade complex by some researchers (eg. Plint et al., in prep. and Craw, 1984) who interpret the units as one continuous sequence of sedimentation and volcanism. MacDonald and Smith (1980) examined the western Highlands volcanic sedimentary complex in the Cape North area and concluded that the low and high grade rocks form a continuous sequence. However, Currie (1982) reported an unconformable contact between the gneisses and overlying low grade rocks of the Jumping Brook Complex. Neale and Kennedy (1975) suggested the presence of an unconformity in the Cape North area.

The Jumping Brook Complex is bounded in the southeast by the Salmon Pool Pluton (365 +10 -5 Ma (Jamieson et al., in press)) and by the Devonian (376 +/- 12 Ma (Keppie and Smith, 1978)) Fisset Brook Formation to the southwest (figure 1.1). To the west the Cheticamp Pluton is located adjacent to the complex (figure 1.1). Ages of 530 +/- 44 Ma (Cormier, 1972), 550 +/- 6 Ma (Jamieson et al., in press), and roughly 550 Ma (Barr et al., in press) have been obtained for the Cheticamp Pluton.

The age of the western Highlands volcanic sedimentary complex is currently under debate. Some workers contend that the complex must be late Precambrian to early Cambrian in age due to the presence of the essentially undeformed Cheticamp Pluton. All known contacts between the complex and the Cheticamp Pluton in the Cheticamp River area are sheared or faulted. However, Barr et al. (in press) report that the Cheticamp Pluton intrudes similar rocks to the southeast. The location of the pluton, which lacks a penetrative fabric, directly adjacent to the metamorphosed and intensely deformed Jumping Brook Complex, also suggests that the complex predates the pluton. However, Currie et al. (1982) obtained an U/Pb age of 439 +/- 7 Ma from zircons in a rhyolite dyke which they believe to have fed the complex. Jamieson (pers comm. 1986) suggests that the linking of the rhyolite dyke with the volcanic layers of the complex is tenuous.

Previously, the western Highlands volcanic sedimentary complex had been correlated with the Hadrynian George River and Forchu Groups, of the south central Cape Breton Highlands. This correlation has been dropped and Jamieson and Craw (1983) recommend the use of local names.

1.4 PREVIOUS WORK

Milligan (1970) reported on the mineralization of two old prospects, Silver Cliff and Core Shack (figure 1.2). Chatterjee (1980) discussed these two along with the Galena Mine prospect (figure 1.2) and also used data from several drill holes. The numerous exploration companies which have worked in the area, beginning in the early 1900's, are outlined in an assessment report by Covey (1979). The land is currently claimed and exploration is continuing.

Craw (1984) mapped the area as part of a larger research project dealing with the metamorphic and structural relationships between the western Highlands volcanic sedimentary complex and the paragneisses to the east. Conrod (1984), Doucet (1983), Currie (1982, in press), and MacDonald and Smith (1980) all examined the western highlands volcanic sedimentary complex or similar lithologies, with similar structural and metamorphic histories, at other locations.

1.5 OBJECTIVES AND APPROACH

The principal aim of this project is to determine the spatial and temporal relationships of the sulphide minerals with the metamorphism and deformation of the host rock. The following questions are addressed:

1. What is the relative timing of the sulphide mineralization, metamorphism, and deformation?

2. What can the metamorphic assemblages reveal about the conditions of metamorphism?

3. What is the relationship between the different structural elements?

4. What is the role of the ductile shear zones with respect to the mineralization?

5. Are there any stratigraphic controls on the sulphide concentrations and if so, what is the significance of these controls?

6. Are the sulphides epigenetic or syngenetic and what are possible environments of deposition?

7. What can geochemistry reveal about the mafic volcanic sequence? How do the analyses compare to those for other mafic volcanic units within the complex?

Conclusions are drawn from field observations, thin section and polished section examinations, as well as geochemical analyses. The extensive accumulation of drill core was not examined due to time constraints.

Mapping at a scale of 1:10000 was carried out over 10 days in late July and early August of 1985. The purpose of the mapping was to record observations of the lithologies and structure within the study area. Several samples were collected from each lithology and thin sections were prepared from chosen specimens. Polished sections were made from samples containing significant amounts of sulphide mineralization or samples which were considered suitable for microprobe analysis. Twenty specimens were collected from a sequence of pillow lavas and prepared for geochemical analysis of the major and minor elements.

CHAPTER TWO

LITHOLOGIES AND FIELD RELATIONS

2.1 INTRODUCTION

The Jumping Brook Complex (Currie, 1982, in press) consists of a succession of metavolcanic rocks overlain by apparently younger metasedimentary rocks. Vague indications of younging direction suggest that the sequence is right way up (in agreement with Craw, 1984 and Currie, in press), however if transposition of the original layering has occurred (see section 3.2 below), this observation may be unreliable.

No upper or lower contacts of the complex have been identified in this area (Covey, 1979). The contact between the metavolcanic and metasedimentary units occurs over an interlayered section and a covered interval of 75 metres on Faribault Brook and over a covered interval of 100 metres on Dauphinee Brook. Due to the lack of upper and lower limits and the possible transposition of original layering, the total thickness of the complex is difficult to determine. Chatterjee (1980) estimates the thickness to be 350 metres, while Covey (1979) gives an estimate of 1000 metres (figure 2.1). The differences in these values may arise from the methods used. Covey (1979) based his estimate on drill core, while Chatterjee (1980) may have used estimates from

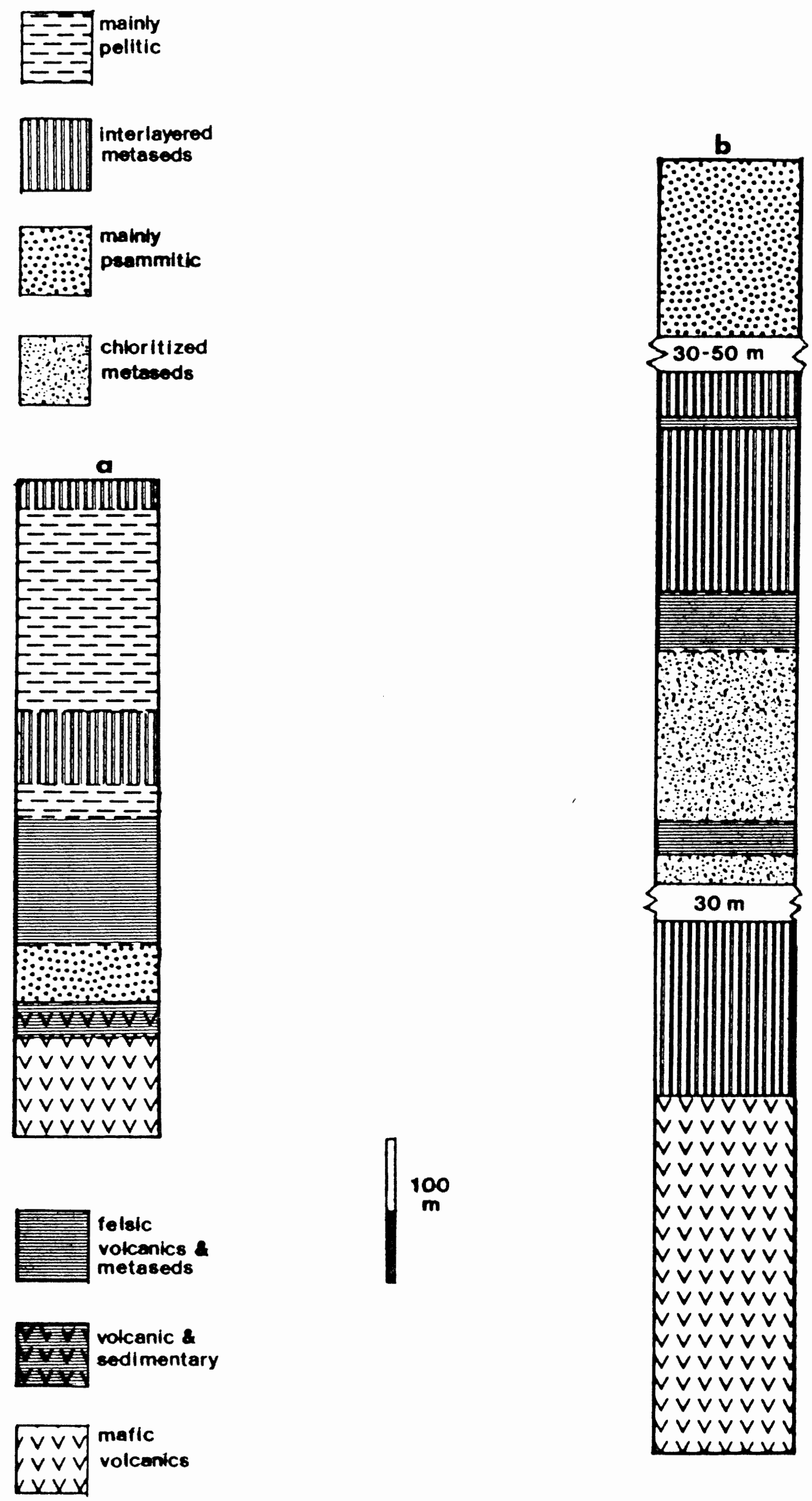

Figure 2.1 Lithologic sections (column A from this study and column B modified after Covey (1979)).

outcrops. It also appears that Chatterjee (1980) only approximated the thickness for the Faribault Brook area, while Covey's estimate includes a larger area. Errors may also arise from calculation of the apparent thickness rather than the true thickness.

A lithologic section along Faribault Brook (figure 2.1) was estimated using the strike and dip measurements along with distances from the base map (figure 1.2). This section gives a rough estimate of 460 metres for the thickness of the section exposed on Faribault Brook.

2.2 METAVOLCANIC UNIT

Volcanic rocks of the Jumping Brook Complex crop out along both Faribault and Dauphinee Brooks (figure 1.2). The volcanic rocks extend from the contact with the metasedimentary sequence and continue past the limits of the study area. The thickness of the unit (within the study area) is estimated at 90 metres (figure 2.1). The metavolcanic unit crops out along Faribault Brook for roughly 1 kilometre, but the essentially horizontal orientation of the layers gives a relatively small value for the total thickness. However, this value may still be exaggerated by tectonic thickening (see section 3.2).

Along Faribault Brook the metavolcanic unit is dominated by a previously unrecognized sequence of pillow lavas in which primary structures are locally preserved. The very fine grained basalts are medium to dark green. Randomly oriented hornblende dominates the mineralogy, while feathery chlorite, plagioclase (+/- quartz) and minor epidote are also present. Opaque minerals make up less than one percent of the grains.

Despite the metamorphism and deformation of the complex distinct elliptically shaped pillows and interpillow material are preserved (figure 2.2). The average size of the pillows is 52*15 centimetres in cross section. The long dimension averages between 1 and 4 metres and is consistently aligned in the north - south direction, parallel to the tectonic fabric. A well preserved lava tube (just south of location Z, figure 1.2) has a cross section of 15*9 centimetres. The pillows locally contain irregular cavities filled by carbonate (figure 2.3) and late veins of carbonate and epidote occur throughout. A well preserved example of radial fractures (figure 2.4) was observed at locality Z, figure 1.2.

No pillow structures were found in the metavolcanic unit along Dauphinee Brook. Here the mafic volcanic rocks are dark green, massive, and fine grained with extensive epidote veining. However, the mineralogy of these rocks is essentially the same as that of the pillow lavas. Hornblende forms the bulk of the sample along with plagioclase (+/- quartz). Chlorite and epidote are minor components, while opaque minerals compose 2 to 3 percent of

Figure 2.2 Elliptically shaped pillow lavas of the mafic volcanic sequence. Arrow 1 indicates the rind and arrow 2 indicates the interpillow material.

Figure 2.3 Carbonate filling an irregular internal cavity in a pillow. White square is 1*1 cm.

Figure 2.4 Radial fractures in a deformed pillow. Arrows indicate orientation of fractures.

the grains. The opaque minerals and hornblende show local alignment. Two brown to pink, porphyritic rhyolite dykes (3-4 metres wide) are located within this unit.

Minor schistose layers are also present within the sequence of pillow lavas. The thickness of these essentially horizontal units ranges from 0.1 to 1 metre. The schistose layers are dominated by a matrix of chlorite and quartz with random porphyroblasts of hornblende, biotite, or chlorite, in order of decreasing abundance. Sulphides comprise 10 to 15 percent of the grains and are intergrown with the hornblende. Deformed quartz - carbonate veins or lenses are present, as in most samples from the mafic volcanic sequence. Contacts between these layers and the pillowed sequence were not observed, but sharp contacts occur between the schistose layers and the amphibolite zones (see section 2.4).

Layers of quartz sericite schist (0.5 to 6 metres thick) occur at the top of the mafic volcanic sequence along Faribault Brook and interlayered with the metasedimentary rocks just above the contact. The fine grained, schistose rocks contain a large proportion of white mica, probably sericite, giving the rock a distinct slippery feel and pearly sheen. Quartz augen and garnet porphyroblasts are present in variable proportions.

Locally, the quartz sericite schists are host to major concentrations of sulphide mineralization (refer to chapter six). Contacts between the quartz sericite schist and the metasedimentary rocks are fairly distinct and sharp, and range from concordant to discordant, suggesting some lateral variation. The lateral change in composition may be produced by deformation (ie. folding) or may be primary.

Direct evidence for the quartz sericite schists being of volcanic origin rather than sedimentary origin arises from petrographic observations. The presence of quartz grains with prismatic terminations and resorption textures (refer to section 4.2) indicates that the unit is a metamorphosed felsic volcanic rock. The terminations would not be preserved in detrital quartz grains. The association with a sequence of mafic volcanic rocks supports the petrographic observations.

2.3 METASEDIMENTARY UNIT

Interbedded pelites, semipelites, and psammites overlie the metavolcanic unit. The individual layers range from 0.5 centimetres to 10 metres thick, with the finer grained layers dominating the sequence. The metasedimentary unit crops out along Faribault Brook for roughly 1200 metres, and along Dauphinee Brook for approximately 1400 metres (figure 1.2). The approximate thickness of the unit, along Faribault Brook, is 370 metres (figure 2.1). This thickness is probably exaggerated by transposition and folding (refer to section 3.2).

Compositional variation is evident within the pelites and semipelites from the color variation in the layering from blue-green to grey-green. The contacts between the 0.5 to 5 centimetre thick layers may be quite sharp or gradational. Gradational contacts in fining up sequences indicate the facing direction is upward, but this interpretation is tenuous owing to deformation.

Mineralogy of the very fine grained pelites is indeterminate in outcrop except for the massive, black lenses which generally contain garnet porphyroblasts. The mineralogy is dominated by very fine muscovite laths. Quartz, garnet, chloritoid, minor tourmaline and sphene are also present. Locally, biotite porphyroblasts are present and chlorite is retrograde. Slightly elongate opaque minerals comprise 1 to 2 percent of the samples. The high proportion of micas in the pelitic layers produces the characteristic silvery sheen on foliation surfaces.

In outcrop tiny quartz augen (0.5 to 2 mm) are locally visible in the slightly coarser grained semipelites. Thin section observations indicate that, in comparison to the pelites, the semipelites are characterized by a higher proportion of quartz (+/- feldspars) and biotite and a lower percentage of muscovite. Porphyroblasts of garnet, minor sphene and tourmaline, and opaque minerals are present as well. Locally, layering within the semipelitic bands is defined by the relative percentage of biotite.

The psammites are fine to medium grained and typically contain distinctive blue quartz grains (1 to 7 mm in size). Locally, the psammites contain porphyroblasts of biotite. Thin section examinations reveal a higher proportion of quartz, plagioclase, K-feldspar, and biotite in comparison to the semipelites. Muscovite is less abundant and garnet, chloritoid, and opaque minerals are still present.

Psammites without quartz augen have a massive, sugary texture. These layers are blue-grey to brownish in color, lacking the greenish tint of the pelites and semipelites. Contacts between the psammites and finer layers appear fairly sharp. Lenses of pelitic material are locally present in the psammites.

2.4 INTRUSIVE UNITS

Fine to medium grained amphibolite layers occur as concordant horizontal zones, 0.5 to 1.5 metres thick, within the pillowed sequence. These layers may represent dykes, sills, or possibly flows. Plagiocalse, hornblende, quartz, and biotite can be distinguished in hand sample, giving the layers a grey to black color. In thin section epidote, carbonate, and retrograde chlorite can also be identified. A fair proportion of sulphide minerals (roughly 10-20%) is typically present. The hornblende and opaque minerals show intergrowth.

Locally, these zones show stretching and alignment of the light and dark minerals. Contacts between this unit and the pillow lavas are sharp, but no chilled margin is evident.

2.5 DISCUSSION

In the Faribault Brook area, the Jumping Brook Complex consists of a metamorphosed sequence of pillow basalts overlain (structurally and/or stratigraphically) by fine to coarse grained sediments. Interbeds of felsic volcanic layers are concentrated at the base of the metasedimentary unit. The recognition of the quartz sericite schist as a felsic volcanic unit is significant due to the association with the sulphide mineralization. This association is discussed in sections 6.1 and 6.3-6.5.

In general, the pelites, semipelites, and psammites are distinguished from each other in outcrop by grain size and the intensity of foliation. The pelites and semipelites are commonly interlayered and dominate over the coarser psammites. In thin section the differences between the rock types are more evident. The relative abundance of quartz increases and micas decreases from the fine to the coarser grained layers.

Evidence of the original mineral assemblages is virtually absent in all of the mafic igneous units. Instead the present mineralogy and texture are entirely metamorphic with hornblende and/or chlorite dominating the samples. The amphibolite layers probably originated as sills or dykes of approximately dioritic composition. The concordant nature of these units implies that they were originally sills. However, the layers may have been discordant prior to deformation. The schistose layers are very similar in bulk composition to the pillow basalts. This suggests that either the schistose horizons represent areas of the pillow sequence where deformation was concentrated (see section 3.10) or the layers originated as tuffaceous deposits erupted from the same source.

CHAPTER THREE

STRUCTURE

3.1 INTRODUCTION

Detailed observations of the structure within the study area were recorded during field mapping. The relationships between the deformation and metamorphism, as well as the deformation and sulphides, were considered carefully during petrographic studies. These relationships are discussed in detail in chapter four and chapter six, respectively.

The numerous and varied structural elements in the area of study indicate polyphase deformation. Relative time relationships can be easily distinguished in the field or by petrographic examination for many structures. The structural features are discussed in order from the earliest to the latest (refer to Figure 4.7).

3.2 ISOCLINAL FOLDING

Bedding - foliation intersections of 30 to 45 degrees (figure 3.2), in an area dominated by bedding parallel foliation (refer to section 3.3), indicates the presence of a mesoscopic to macroscopic isoclinal fold hinge at the Core

Shack property. The bedding - foliation intersection is present both at the top of the outcrop and near the base, indicating a hinge thickness of more than 10 metres. The orientation of the intersection angle indicates that the fold closes to the west. Craw (1984) also describes an isoclinal fold hinge in lower Faribault Brook which is 10 metres wide, perpendicular to the limbs.

Smaller, mesoscopic, isoclinal folds (wavelength 1-2 centimetres) are most obvious in the sequences of interlayered pelites and semipelites. These folds show axial planes which are consistently parallel to the foliation and compositional banding. Intrafolial, isoclinal folds are observed in outcrop.

On a microscopic scale, isoclinal folds are observed in both the metasedimentary and metavolcanic sequences. Veins of quartz and/or carbonate are isoclinally folded with the axial planes parallel to the foliation. Isoclinally folded quartz veins are also observed in outcrop.

The presence of intrafolial folds and the bedding parallel foliation strongly suggests that transposition of the original layering has occurred (Davis, 1984). The limbs of the isoclinal folds have been transposed and rotated into the foliation. The transposition causes the original layering to be repeated throughout, consequently increasing the apparent thickness of the sequence. However, no obvious repetition of distinctive layers is observed.

3.3 FOLIATION

The pervasive foliation, S1, trends closely parallel to the compositional layering (possibly S0 or the result of transposition) of the metasedimentary package (figure 3.1). The foliation is axial planar to the isoclinal folds and truncates the layering in fold hinges (figure 3.2). The foliation is best defined in the mica rich pelites and semipelites, whereas the psammitic layers show the cleavage to a lesser degree. Microscope observations show that tiny laths of muscovite, along with fine grained quartz, define the foliation in the pelites. The semipelites and psammites contain increasing proportions of larger quartz (+/- feldspar) grains, thus reducing the intensity of the foliation. In the psammitic layers the micas anastomose around quartz augen (figure 3.3).

Locally, the foliation is fairly well developed in the metavolcanic unit, especially in the schistose layers. Petrographic observations of the pillow lava sequence indicate a nearly random arrangement of grains with only local alignment. However, a strong mesoscopic lineation and a mesoscopic foliation, defined by flattening of the pillows, are observed in outcrop. The amphibolite units locally contain aligned hornblendes and sulphides which define a weak to fair foliation. Layering in the schistose zones is defined by aligned hornblendes and matrix chlorite and quartz.

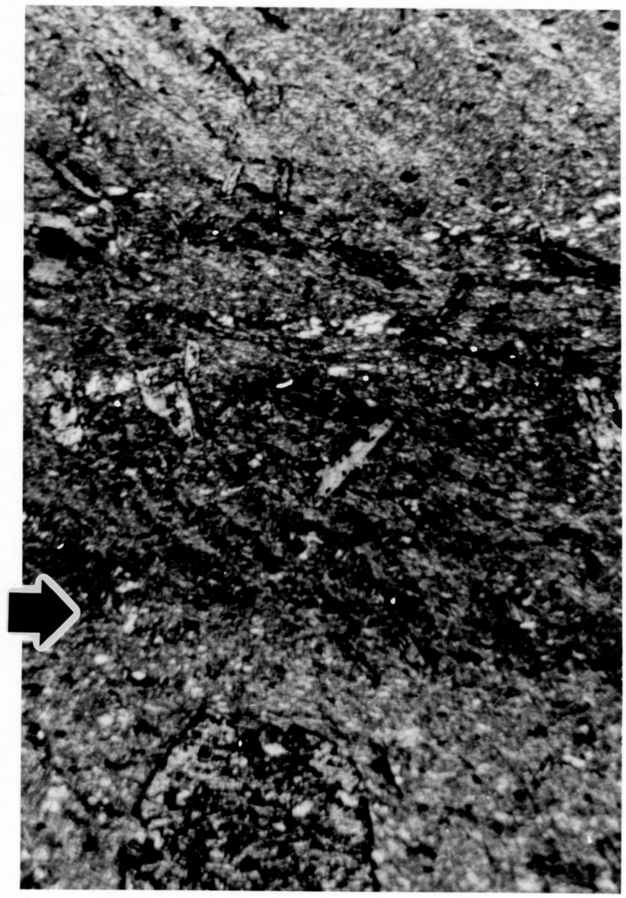

Figure 3.1 Bedding parallel foliation (S1) with the later crenulation (S2) at a high angle. The foliation is oriented E-W and the crenulation NW-SE. The upper layer is pelitic and the lower is semipelitic. The contact trends E-W and is indicated by the arrow. Field of view is 5*3.4 mm.

Figure 3.2 Sample from the hinge zone at the Core Shack location. Foliation cuts the compositional layering of the metasedimentary unit. The dark layer is pelitic and the light layer is semipelitic. Field of view is 5*3.4 mm.

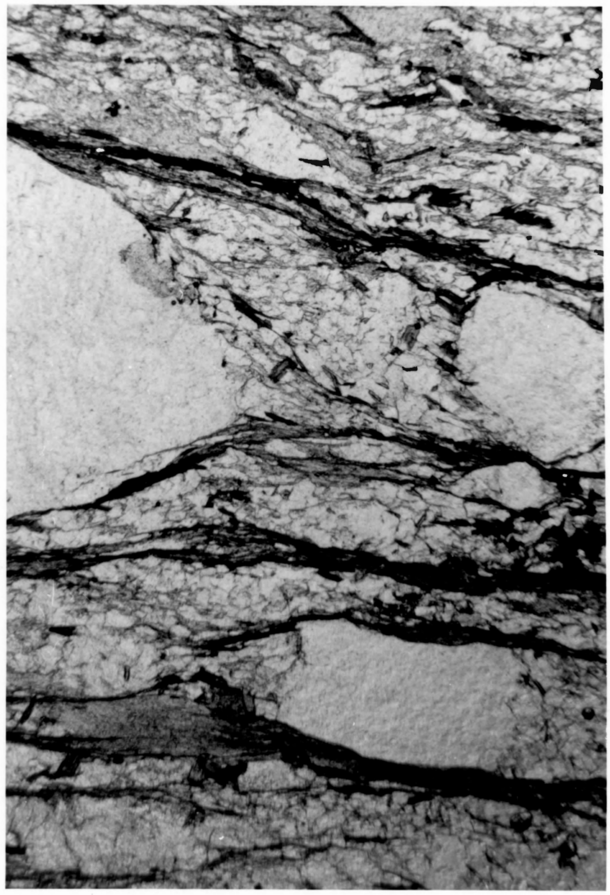

Figure 3.3 Anastomosing foliation in the coarser psammitic layers of the metasedimentary package. The intensity of the foliation is decreased due to the presence of the quartz and feldspar augen. The field of view is 5*3.4 mm.

The orientation of the foliation varies somewhat due to the later folding (section 3.5). Strikes ranging from NE to SE are common, while the dips are between 10 and 40 degrees.

3.4 DUCTILE SHEARING

The ductile shear zones are 0.1 to 1.0 metre thick and occur at low angles to the foliation. Most are subhorizontal as well. Retrograde chlorite is abundant and locally large crystals of hornblende are present. Petrographic examination of a sample from a shear zone reveals a very fine grained assemblage of hornblende, chlorite, epidote, and recrystallized quartz. Layers of chlorite and hornblende are strictly aligned in the plane of shearing, while other zones have a less ordered arrangement of grains. C and S planes are present. An isoclinal fold with the axial plane parallel to the plane of shearing, is also visible in thin section. Boudinaged quartz veins typically occur within the shear zones. Locally, these shear zones are host to significant concentrations of sulphide minerals (section 6.6).

Zones of ductile shearing occur intermittantly over a distance of roughly 600 metres along Faribault Brook (from X to Y, figure 1.2). A 1 metre wide zone of intense shearing is located to the south just outside the area of study. It is unclear whether the observed zones are part of the same shear or represent a system of anastomosing shear zones.

3.5 UPRIGHT FOLDING

A later period of deformation produced gentle to open, upright, similar style folds. A macroscopic, north trending antiform is defined by the contoured stereogram of the S-pole diagram for the foliation measurements over the entire metasedimentary unit (figure 3.4). No evidence of this fold is found in outcrop. The stereogram plot indicates that the fold axis is plunging gently to the north. Other workers have also indicated the presence of such a structure, both in this area (Craw, 1984) and farther to the north (Conrod, 1984).

Mesoscopic folds of this generation are present throughout the metasedimentary unit, but they are not as common in the metavolcanic unit. The wavelength varies from 1 to 2 centimetres up to 10 metres and the amplitude ranges between 1 centimetre and 2 metres. The interlimb angle is frequently so large that the folds merely appear to be very low amplitude warps in the foliation. The axial plane is within 20 degrees of vertical. Orientation of the fold axes is variable, but most are distinctly parallel or perpendicular to the fold axis of the major antiform. Craw (1984) suggests that early formed fold axes were rotated towards the stretching direction by post metamorphic

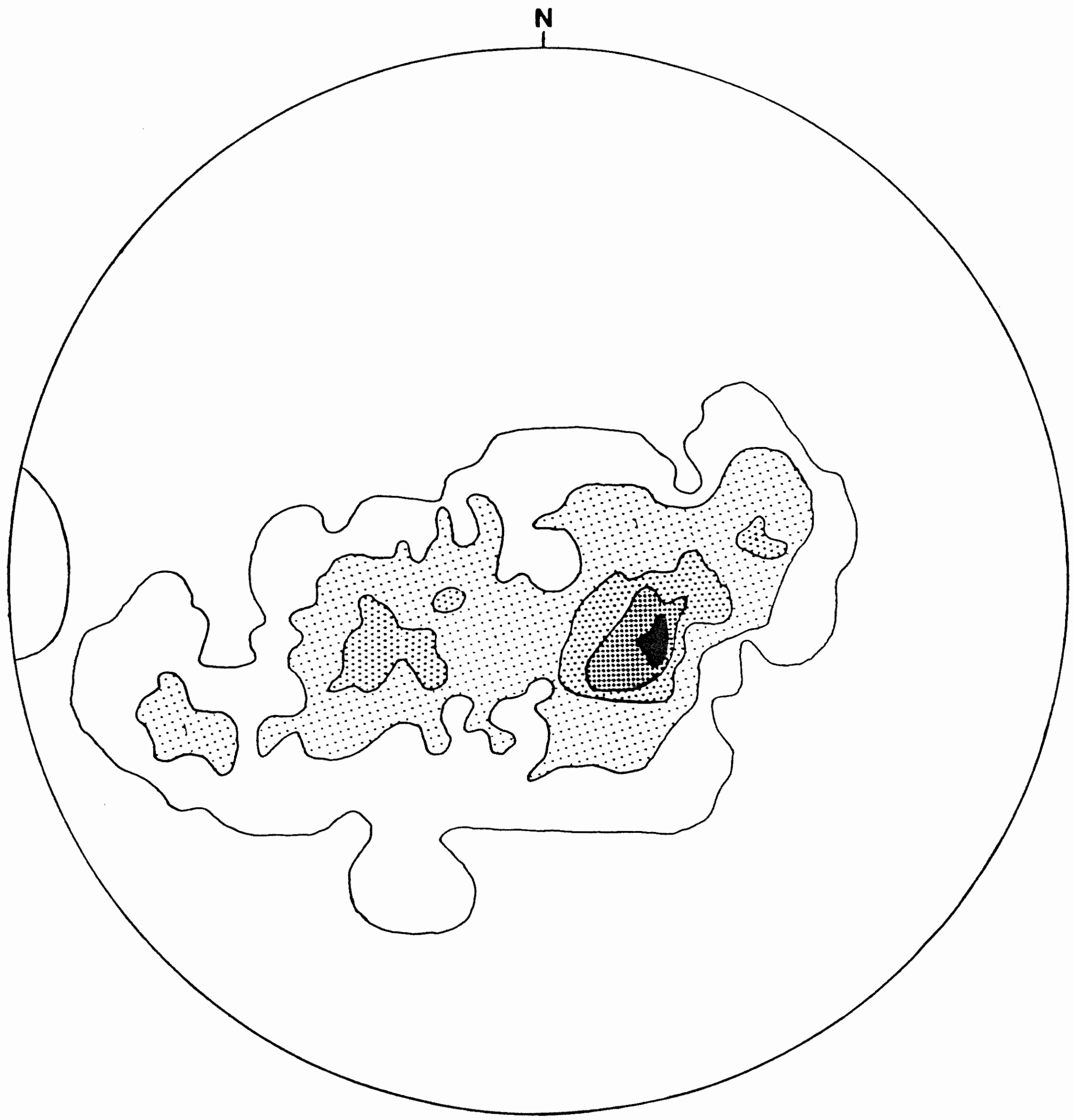

Figure 3.4 Contoured equal area plot of foliations from the metasedimentary unit.
contours = 1,4,8,12, and 16 percent
maximum value = 17.8 percent
90 points

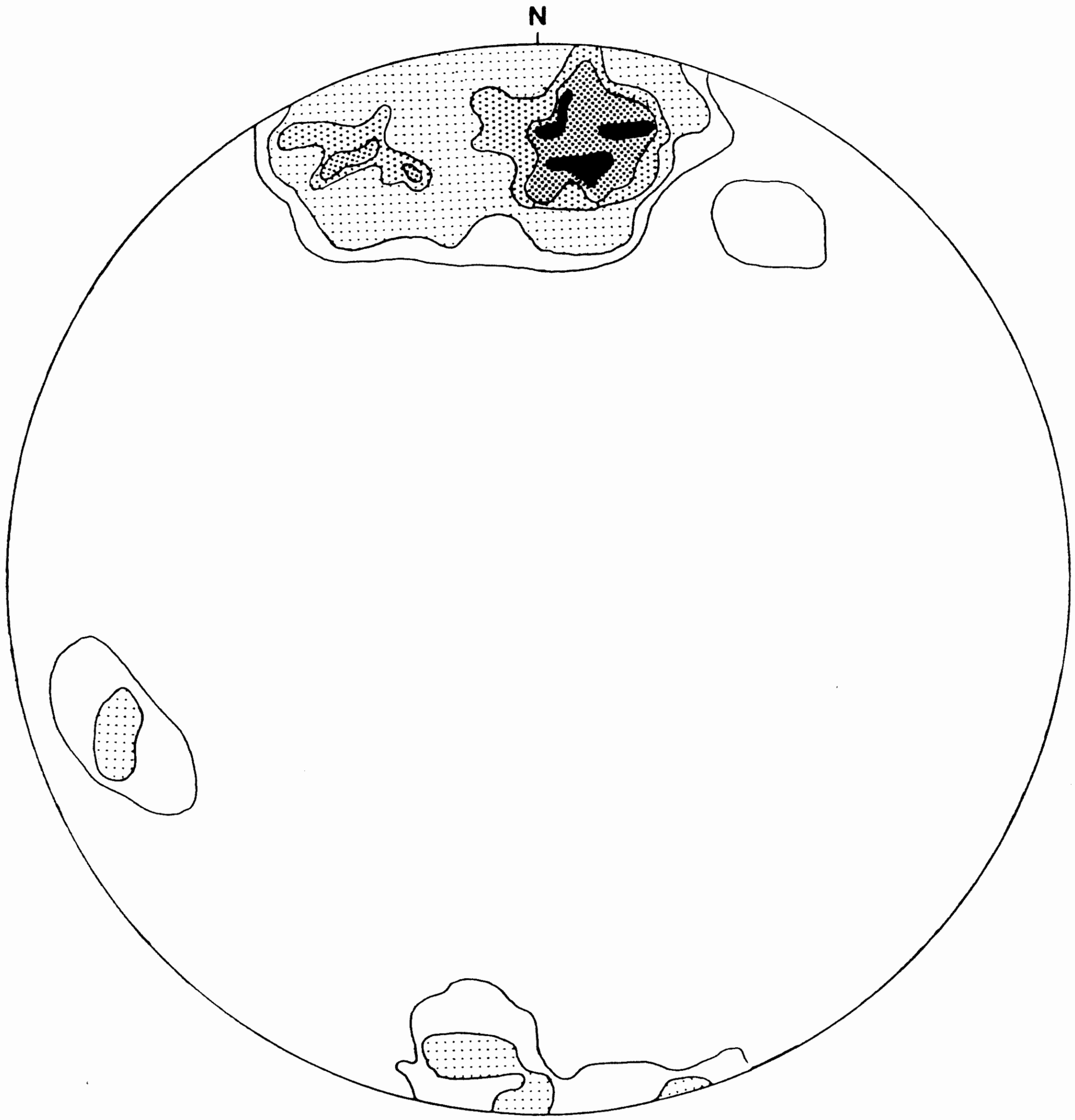

Figure 3.5 Contoured equal area plot of mineral lineations and crenulation axes.
contours = 1,5,10,15, and 20 percent
maximum value = 30 percent
30 points

deformation.

3.6 CRENULATIONS AND LINEATIONS

A set of gently northward dipping crenulations defines the development of a second cleavage, S2, in the pelitic units. The parallel laths of muscovite in the pelites are folded by the later crenulation. The consistency of the crenulation orientation is demonstrated by the stereogram (figure 3.5). The crenulations are also found in the semipelitic unit, but are rare in the psammites. Locally, the schistose layers of the metavolcanic sequence show good crenulation patterns.

Mineral lineations, generally parallel to the crenulation fold axes, are defined by quartz in the psammitic layers, sheet silicates in the pelites and semipelites, and by hornblende or chlorite in the pillowed horizon. Both the lineations and crenulation axes are oriented parallel to the fold axis of the macroscopic antiform.

3.7 KINKING

A series of mesoscopic east-west trending kinks with wavelengths ranging between 1 and 40 centimetres occur throughout the metasedimentary unit. North - south trending kinks are not as common. These kinks commonly show fracturing along the fold axis. The fracturing may initiate the kinking or it may postdate the kinks. Craw (1984) suggests that the kinking may be related to late stage faulting.

Small kinks, S3, (0.1 millimetres wide) can be observed in thin section. The kinks are observed to refold the crenulations. Fracturing and brecciation are found in two wider (3.5 millimetres) kinks or faults.

3.8 FAULTING

Numerous near vertical fault surfaces are present within the study area, but their significance and extent are difficult to determine. Some faults are large features, 10 to 15 metres in extent, with breccia or gouge, and some are only small planes showing slickensides. Several faults are assumed to juxtapose different lithologies, however this was inferred from compositional and structural data and not directly observed.

The steep fault planes often trend close to north - south or east - west (+/- 20 degrees), while dips are to the west or south in most cases. Slickensides are oriented roughly 20 degrees below the horizontal. No marker horizons were present to allow for estimation of the amount of offset along the faults.

An east - west trending fault truncates the mineralized zone at the Core Shack property. This is a reverse fault with the mineralized block upfaulted by as much as 350 metres (Covey, 1979). Covey (1979) also noted the north - south and east - west alignmemt of faults. (Note - faults mapped by Covey (1979) are indicated on figure 1.2.) Two major north - south trending faults are the Silver Cliff fault and the Faribault Brook fault. The vertical Silver Cliff fault is a brittle shear zone which lies to the east of the Silver Cliff showing (Covey, 1979). It crops out, within this study area, to the northeast on the main branch of Dauphinee Brook (figure 1.2) where a rhyolite dyke in the metavolcanic unit is cut by an intense fracture zone 3 to 5 metres wide. The near vertical Faribault Brook fault is a 10 to 20 metre wide shear zone which can be seen in several outcrops in the central part of Faribault Brook (Covey, 1979). This may account for the north - south trending fault planes recognized in this study. An east - west fault cuts across the Silver Cliff fault suggesting that the north - south faulting predates the east - west faults (Covey, 1979). East - west faults are also observed to affect Mississippian rocks along the coast, indicating that the age of faulting is partly post - Mississippian (Covey, 1979).

3.9 BRITTLE SHEARING

The brittle style shear zones occur at a high angle to the foliation and are roughly oriented in an east - west direction. The vertical shears contain zones of brecciation from 5 to 40 centimetres wide and were observed to continue for only 1 to 3 metres. Unlike the ductile shear zones these show no significant amounts of sulphide mineralization. The sense of movement was determined to be sinistral in most cases.

3.10 DISCUSSION

Deformation of the western Highlands volcanic sedimentary complex has been polyphase. At least three episodes of deformation can be discerned from the field and petrographic observations (refer to figure 4.7). The oldest period of deformation, D1, produced intense isoclinal folding and the associated axial planar foliation. Both the foliation and isoclinal folds were later deformed by mesoscopic to macroscopic upright folds. Crenulations and lineations are roughly parallel to the axis of the major antiform. Therefore, it is probable that all three formed during the same period of deformation, D2. The pillow basalts show re-alignment parallel to the axis of the antiform.

The faults, kinks, and brittle shearing show a prominent east - west orientation (although the faults trend north - south as well). The brittle structural style and the similar orientation implies that these structures all formed during a late period of deformation, D3.

The timing of the ductile shearing is somewhat equivocal in relation to the other structural events. However, the orientation and the ductile nature of the shearing suggests that it developed during the earliest, most ductile stage of deformation, D1. This suggestion is supported by the very gentle, open folds, probably of D2 age, which deform the shear zones. The early presence of the shear zones is also supported by the random orientation of hornblende porphyroblasts which suggests metamorphism peaked after shearing.

The deformation appears to have been concentrated in the less competent layers of both the metasedimentary and metavolcanic units. The pelites and semipelites have developed the foliation to a much greater degree than the psammites, just as the shearing is concentrated in the schistose layers of the metavolcanic unit. The more competent pillow basalts show only a mesoscopic foliation, defined by the flattening of the pillows, and a lineation, but no microscopic foliation.

Craw (1984) proposes that the pervasive deformation of this area resulted from the east to west stacking of a low, medium, and high grade belt. The rocks of this study area lie within the low grade belt which Craw suggests is part of the upper limb of a (now) recumbent, isoclinal fold which closes to the west. The westward closure of isoclinal folds was noted in this study and by Currie (in press). Craw's interpretation of structure implies that the mafic volcanic rocks are the oldest unit and that the sequence has not been overturned.

CHAPTER FOUR

METAMORPHISM

4.1 INTRODUCTION

Over 100 samples were collected from the various units which are found within the study area. Thin sections were cut from 21 samples and polished sections from 11 samples. The purpose of the petrographic study was to determine the phases present in the metamorphic assemblages and examine the textural relationships. Petrographic descriptions of the individual thin sections are given in appendix A.

4.2 METAMORPHIC ASSEMBLAGES AND TEXTURES

Determination of the metamorphic assemblages gives an estimation of the pressure and temperature conditions of metamorphism. An examination of the textural relationships between the metamorphic minerals and the fabric development can indicate the relative timing of metamorphism and deformation.

4.2.1 METAVOLCANIC UNIT

The pillow basalts show no indication of the original mineral assemblage. The metamorphic assemblage is dominated by laths of hornblende, plus plagioclase (+/- quartz), chlorite, and epidote. The plagioclase and quartz are difficult to distinguish between, however it is probable that quatrz is a very minor component, if present at all, due to the absence of quartz in the CIPW norm values (Appendix B). Minor opaque minerals are also present. Generally, the very fine grained minerals are arranged randomly, however some random aggregates are surrounded by a weak foliation.

The metabasites from Dauphinee Brook are slightly coarser grained and show a weak foliation. The hornblendes range from aligned to random. Plagioclase (+/- quartz), epidote, and a few opaque grains are present as well.

The schistose zones contain a metamorphic assemblage consisting of hornblende, chlorite, quartz, epidote, and plagioclase. The fairly well developed foliation is defined by hornblende, chlorite, and quartz. The hornblende ranges from idioblastic to xenoblastic and contains random inclusions of quartz. The porphyroblasts are commonly aligned in the foliation, but post-tectonic growth is also evident. A fair proportion of opaque minerals are present. The opaque minerals are aligned parallel to the hornblende and the two are locally intergrown. Quartz - carbonate veins are oriented parallel to the foliation.

The quartz sericite schist (felsic volcanic) has a metamorphic assemblage which includes quartz, sericite, garnet, and large grains of muscovite. A variable proportion of sulphide minerals is observed. The pervasive foliation is defined by the sericite and slightly elongated quartz grains.

The quartz is present as large augen, as well as fine grains in the matrix. The foliation is distinctly bent around the blocky to elliptical grains. The quartz is consistently aligned with the long dimension parallel to the foliation (figure 4.1). Several quartz clasts show distinct prismatic terminations, and resorption textures are found in most grains (figure 4.1).

Porphyroblasts of garnet that overgrow the matrix fabric show curved inclusion trails of quartz which have the same shape and same orientation as the matrix crenulations. The garnets apparently nucleated in the mica rich zones and grew during a period of flattening (eg. Bell, 1985). The foliation bends around the grains. The garnets are fractured and the boundaries are commonly irregular. Large flakes of muscovite are associated with the garnet. In mineralized zones of the quartz sericite schist the garnet grew around the sulphide grains (figure 4.2).

The potassic composition along with the presence of spessartine rich garnet (up to 24% MnO (Craw, unpub. data)) suggest an original compositional difference between these

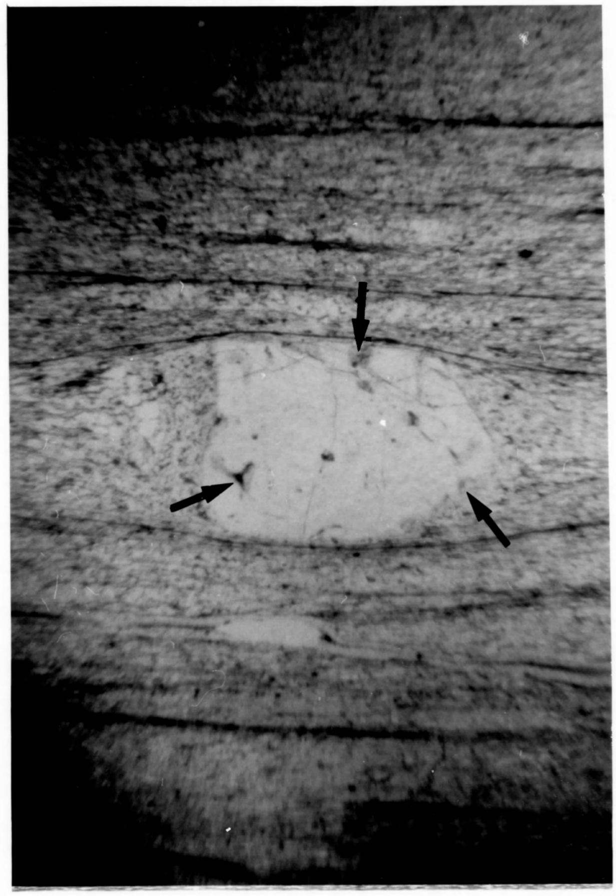

Figure 4.1 Quartz augen in the quartz sericite schist showing alignment with the long axis parallel to the foliation. Note the prismatic termination and the evidence of resorption (indicated by the arrows) which indicate that this unit is a volcanic layer and not sedimentary. The field of view is 9*6 mm.

Figure 4.2 Garnet nucleated and grew around the sulphide minerals in this sample of the quartz sericite schist from Galena Mine. The same texture is found in samples from the Silver Cliff showing. The field of view is 5*3.4 mm.

layers and the metasedimentary rocks. This supports the evidence for the quartz sericite schist being of felsic volcanic origin.

4.2.2 METASEDIMENTARY UNIT

The metamorphic assemblage of the pelitic layers consists of muscovite, quartz, garnet, and chloritoid, +/- biotite and chlorite. Opaque minerals, minor tourmaline and sphene are present as well. The preferred orientation of the fine grained muscovite and slightly elongated quartz defines the pervasive foliation. The later crenulation is observed to deform the foliation and is the dominant fabric in some samples. No evidence of original or metamorphic layering is present in the pelites.

Idioblastic to subidioblastic porphyroblasts of garnet overgrow the foliation. The poikilitic garnets contain inclusion trails of quartz which overgrow the matrix fabric and mimic the crenulation pattern (figure 4.3). Locally, the foliation is slightly deflected by the garnets. Idioblastic to subidioblastic porphyroblasts of chloritoid occur parallel to the foliation or randomly oriented. The chloritoid contains hourglass shaped inclusion trails of quartz. Both simple and penetration twins are observed.

Biotite is generally absent from the pelitic zones, but locally random porphyroblasts with irregular boundaries are

Figure 4.3 Quartz inclusion trails in garnet from a semipelitic layer. The garnet has overgrown the matrix fabric and the inclusion trails mimic the crenulation pattern. The inclusion trails are continuous with the matrix. The foliation (S1) is oriented E-W and the crenulation is trending NW-SE. The field of view is 5*3.4 mm.

present. Chlorite is observed only as a retrograde phase after muscovite.

The semipelitic metamorphic assemblage consists of quartz, muscovite, biotite, plagioclase, and garnet, +/- chlorite. K-feldspar (detrital ?), opaque minerals, minor tourmaline, and sphene +/- apatite can also be observed. A significant amount of carbonate is present in a few samples. Layering in the semipelites is defined by the relative abundance of quartz and muscovite. It is unclear whether this layering represents a primary difference in composition or is the result of metamorphic segregation. The foliation is defined by muscovite and elongate grains of quartz, as in the pelites. Locally, the later crenulation is well developed. Both are most prominent in the muscovite rich layers.

Quartz and feldspar form small augen with well developed strain shadows of quartz and muscovite. Both plagioclase and K-feldspar show some degree of alteration, probably to sericite or another white mica. Biotite occurs both in the matrix and as random or aligned porphyroblasts. The grains are unaltered or relict with irregular boundaries and chlorite alteration.

Porphyroblasts of garnet range from idioblastic with few inclusions to xenoblastic with numerous large inclusions. The idioblastic garnets are found within the muscovite rich layers, while the xenoblastic grains occur in the quartz rich zones. The inclusion trails are continuous with the matrix and mimic the matrix fabric.

The metamorphic assemblage of the psammitic layers includes quartz, muscovite, plagioclase, biotite, garnet, and chloritoid. K-feldspar (detrital ?), opaques, retrograde chlorite, and minor sphene +/-apatite +/- tourmaline are present as well. Vague indications of layering are present in the matrix of quartz and micas. The foliation is less well developed due to the presence of relatively large quartz and feldspar augen. Muscovite and biotite form an anastomosing pattern around the augen (figure 3.4).

Augen of quartz and feldspar, with well formed strain shadows, are abundant. The quartz is present as whole clasts or polygonal aggregates. The plagioclase and K-feldspar occur as rather blocky grains with asymmetric strain shadows which indicate a small amount of rotation. The degree of alteration of the feldspars, to white mica, varies from grain to grain. Biotite is present both in the matrix and as irregular porphyroblasts which overgrow the foliation. Retrograde chlorite replaces muscovite as well as biotite.

Porphyroblasts of garnet are fractured perpendicular to the flattening direction. Quartz inclusion trails indicate that the garnets have overgrown the matrix fabric. Minor chloritoid is present as irregular porphyroblasts with few quartz inclusions. Both the garnet and chloritoid have nucleated in the quartz strain shadows or on the quartz grains and continued to grow along the foliation planes where the micas are concentrated (figure 4.4).

4.2.3 INTRUSIVE UNITS

The metamorphic assemblage of the amphibolite zones consists of hornblende, plagioclase, quartz, epidote, sulphides, +/- chlorite. The degree of foliation in the amphibolites varies from almost none to fairly pervasive. The alignment of dark and light minerals defines the foliation.

Idioblastic hornblende commonly overgrows the foliation, while grains of subidioblastic to xenoblastic hornblende are aligned. Locally, the hornblendes contain quartz inclusions and show fractures perpendicular to the direction of elongation. Opaque minerals are fairly abundant and commonly are intergrown with the hornblende (figure 4.5).

Sheaths of biotite occur parallel to the xenoblastic hornblendes. Retrograde chlorite is commonly present. Both quartz and plagioclase show undulose extinction. The plagioclase contains inclusions of quartz and is partially altered to a white mica.

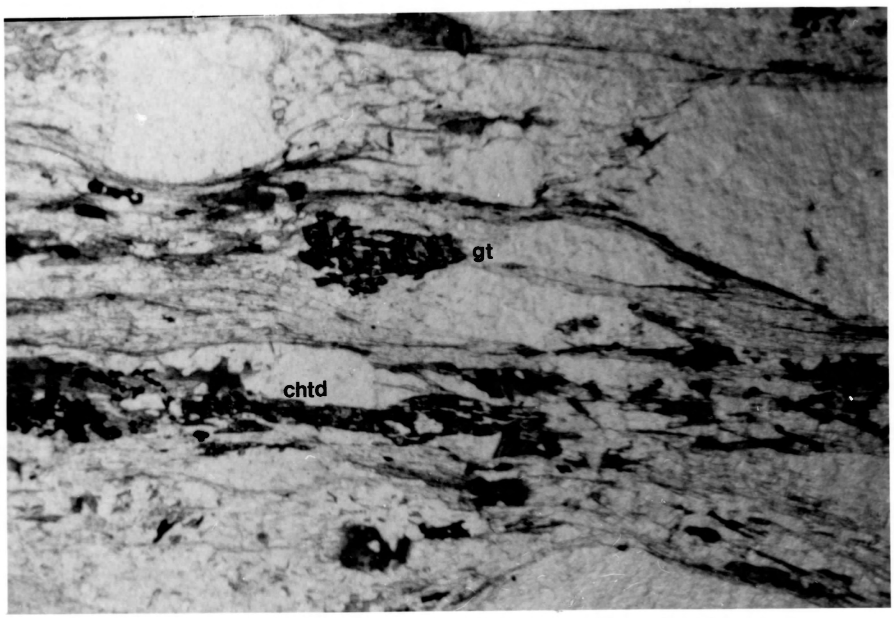

Figure 4.4 Both garnet and chloritoid have nucleated and grown in the quartz strain shadows or on the quartz grains. The porphyroblasts have continued to grow out into the foliation, during a period of flattening, along the mica rich zones of the psammites. The field of view is 5*3.4 mm.

Figure 4.5 Opaque minerals are intergrown with the hornblende in this sample of an amphibolite layer. This texture is also observed in the schistose layers. The field of view is 5*3.4 mm.

4.3 DISCUSSION

Craw (1984) determined that the plagioclase composition is oligoclase (An 20-28) for the metasedimentary unit and An 19-22 for the metavolcanic unit. The coexistence of garnet and oligoclase, in the metasedimentary unit, indicates a metamorphic grade in the lower amphibolite facies (Turner, 1981). The presence of chloritoid is consistent with lower amphibolite facies metamorphism, as it can not persist above this grade (LaTour _et al._, 1980). The metamorphic assemblage in the metavolcanic sequence includes hornblende, clinozoisite, plagioclase (An 19-22), +/- chlorite. The presence of hornblende and plagioclase (An >20) indicates a metamorphic grade in the amphibolite facies (Turner, 1981). However, clinozoisite and chlorite do not persist above the greenschist facies (Turner, 1981). The hornblende and chlorite appear to be in equilibrium in some samples, therefore the assemblage implies a metamorphic grade near the greenschist - amphibolite boundary.

Craw (1984) suggests temperatures ranging between 500 °C and 650 °C with low to medium pressures prevailed during metamorphism. While Currie (in press) proposes similar PT conditions of 450 °C and 3 kilobars to 650 °C and 4 kilobars. Both researchers agree that the metamorphic grade increases from west to east within the Jumping Brook Complex. The petrogenetic grid shown in figure 4.6 shows the restrictions on the temperature which are imposed by the presence of chloritoid and garnet +/- biotite and the lack of staurolite. The reaction lines on the PT grid suggest that the temperature range is between 425°C and 575°C.

The timing of metamorphism with respect to deformation can be estimated from petrographic observations. The preferred orientation of the muscovite laths indicates the syntectonic growth of this mineral and initiation of metamorphism during development of the foliation. Fine laths of biotite are aligned in the foliation, while post-tectonic biotite porphyroblasts are common in the semipelitic to psammitic layers. The porphyroblasts of chloritoid range from aligned to random and the foliation is only deflected to a small degree. This implies that chloritoid growth occurred late syntectonic to post-tectonic with respect to the development of the pervasive foliation, S1.

The quartz inclusion trails in the garnet porphyroblasts mimic the matrix crenulation and the foliation is only slightly deflected by the grains. Therefore, the growth of garnet is late syntectonic to post-tectonic with respect to the crenulation, S2. The peak metamorphic assemblage consists of garnet and chloritoid +/- biotite, thus indicating the peak of metamorphism occurred during or after the development of S2. Continuation of metamorphism is indicated by the presence of random biotite and a few garnet porphyroblasts which overgrow S2.

The tightening up of S2 crenulations, which is evident

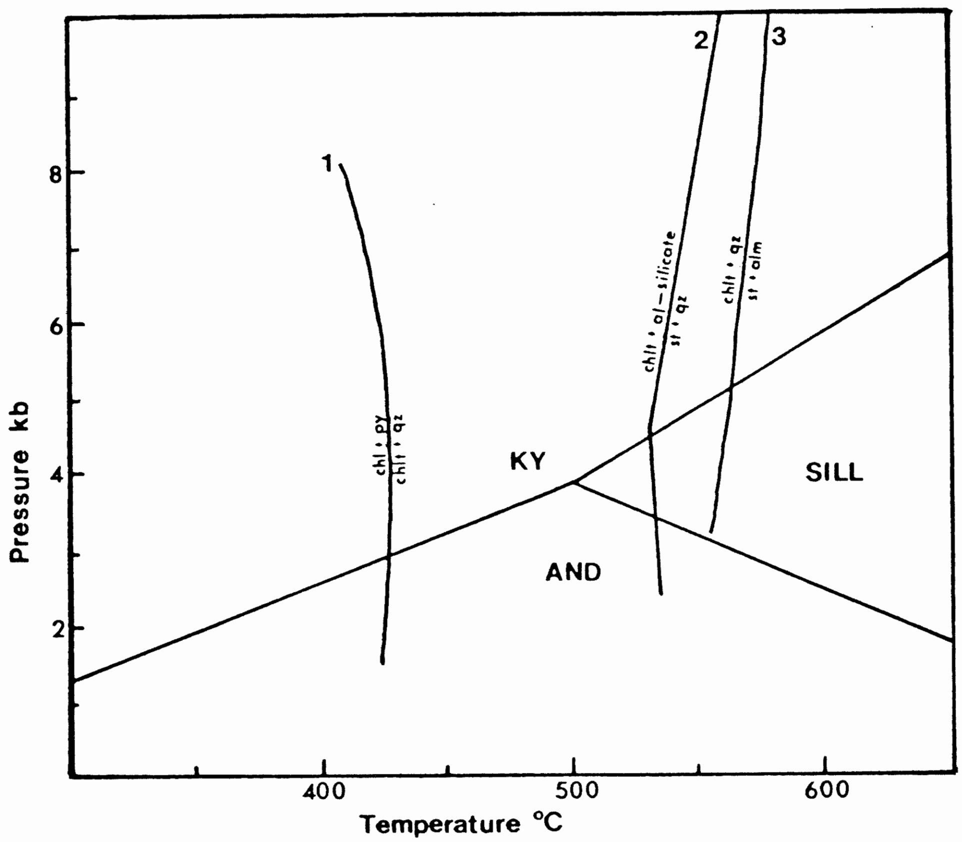

Figure 4.6 The petrogenetic grid shows reactions which control the presence of chloritoid in pelitic rocks. The grid suggests that the temperature of metamorphism must have ranged between 425 °C and 575 °C. The aluminum silicate triple point is from Holdaway (1971). Reaction 1 is from Hoschek (1969) and reactions 2 and 3 are taken from Bickle and Archibald (1984).

GEOLOGIC HISTORY

EVENT	FABRIC	METAMORPHIC MINERALOGY	COMMENTS
Deposition	compositional layering		deposition of sulphides
D1 - F1	isoclinal folds		transposition of layering
	ductile shear zones		remobilization of sulphides
- S1	axial planar foliation	qz - ms - chlt +/- bt	
D2 - F2	meso to macro upright folds		modification of mineralized layers
- S2	crenulation	gt - bt	
- L2	lineations		
D3 - F3	faults, kinks brittle shears		brecciation of sulphides
- S3	kinks and/or crenulations		

Figure 4.7 A summary table showing the relationship between the deformation, textures, and metamorphic mineral assemblages. The deposition and deformation of the sulphide minerals are discussed in chapter six.

in some samples, may be a continuation of S2 or the result of late kinking, S3. At least some crenulations or kinks are post peak metamorphism, indicating the presence of S3. The table shown in figure 4.7 summarizes the episodes of deformation and the fabrics and metamorphic assemblages associated with each episode.

The relationship between metamorphism and deformation within the metavolcanic unit is not as clear due to the variable degree of foliation between the different lithologies and within one lithology. In the amphibolite layers, hornblende and sulphides +/- biotite range from random to fairly well aligned. The schistose layers typically show a fair to well developed foliation, while the pillow basalts contain randomly oriented hornblende with only local alignment. In general, the metamorphic minerals show syn- to post-tectonic growth with respect to S1. S2 generally is not evident in the igneous units.

CHAPTER FIVE

GEOCHEMISTRY

5.1 INTRODUCTION

Major, minor, and trace element compositions of 20 samples from the sequence of pillow basalts were determined by X-ray fluorescence at St. Mary's University, Halifax, Nova Scotia. The original analyses are listed in Appendix B with total Fe calculated as FeO. The CIPW norm calculations are also given in the appendix.

The major, minor, and trace element concentrations are plotted on several discriminant diagrams. Together these diagrams indicate a possible tectonic origin for the unit. A comparison is made between these analyses and those for other mafic volcanic rocks from the western Highlands volcanic sedimentary complex and related units.

5.2 GENERAL CHEMISTRY

The samples are chiefly olivine or hypersthene normative basalts (refer to appendix B). However, the high values of olivine in many samples may be the result of the calculation of total iron as FeO. The only quartz normative sample has a very high loss on ignition and much lower Na_2O and K_2O levels, probably indicating alteration. In general, the loss on ignition values are fairly high. The levels of both Ni and Cr are quite high for basaltic rocks and the levels of incompatible elements such as K_2O, Rb, Ba, Zr, and Nb are very low.

5.3 DISCRIMINANT DIAGRAMS

The compositions of the pillow lavas are plotted on the TiO_2-K_2O-P_2O_5 diagram of Pearce et al. (1974). Potassium is generally considered to be a mobile element, but it appears to be fairly constant in this unit. Figure 5.1 shows that the TiO_2 and P_2O_5 ratios are very consistent, while the relative percentage of K_2O varies to a small degree. All the samples plot inside the oceanic field.

The next diagram shows a plot of TiO_2 versus Zr. Both of these elements are considered immobile during metamorphism. The fields separating the oceanic alkali basalts and oceanic tholeiitic basalts in figure 5.2 were defined by Floyd and Winchester (1975). The samples plot in a straight line trend within the tholeiitic field. Floyd and Winchester (1975) suggest other plots, involving Nb, Y, and P_2O_5 along with TiO_2 and Zr, which can also distinguish between alkaline and tholeiitic basalts. The pillow basalt samples all plot within the tholeiite field for a plot of

Nb/Y versus Zr/P2O5. However, the Nb values for the pillow basalts are very low and therefore subject to significant error. Thus the plot is not shown. But even considering the maximum possible error in the Nb values the samples would still plot within the tholeiitic field.

Pearce (1976) devised a method for statistical analysis of major element patterns in basalts. Three discriminant functions, F1, F2, and F3, are calculated for the major elements. The discriminant functions are linear combinations of the original oxide weight percent values with a different set of eigenvectors for each function. Figure 5.3 shows a plot of F2 versus F1. The samples straddle the dividing line between the ocean floor basalt field and the low potassium tholeiite/calc-alkaline basalt field. This diagram can not differentiate between low potassium tholeiites and calc-alkaline basalts, but Pearce (1976) suggests that a plot of F3 versus F2 will separate the low potassium tholeiites, calc-alkaline basalts, and shoshonites. The samples plot in both the low potassium tholeiite and ocean floor basalt fields for this diagram as well.

Figure 5.4 is a plot of TiO2-MnO-P2O5. The fields are defined by Mullen (1983). A small degree of scatter is shown by the samples indicating minor mobilization, probably in the MnO. However, all the samples plot within the island arc (low potassium) tholeiite field.

The immobile elements Ti, Zr, and Y are used for

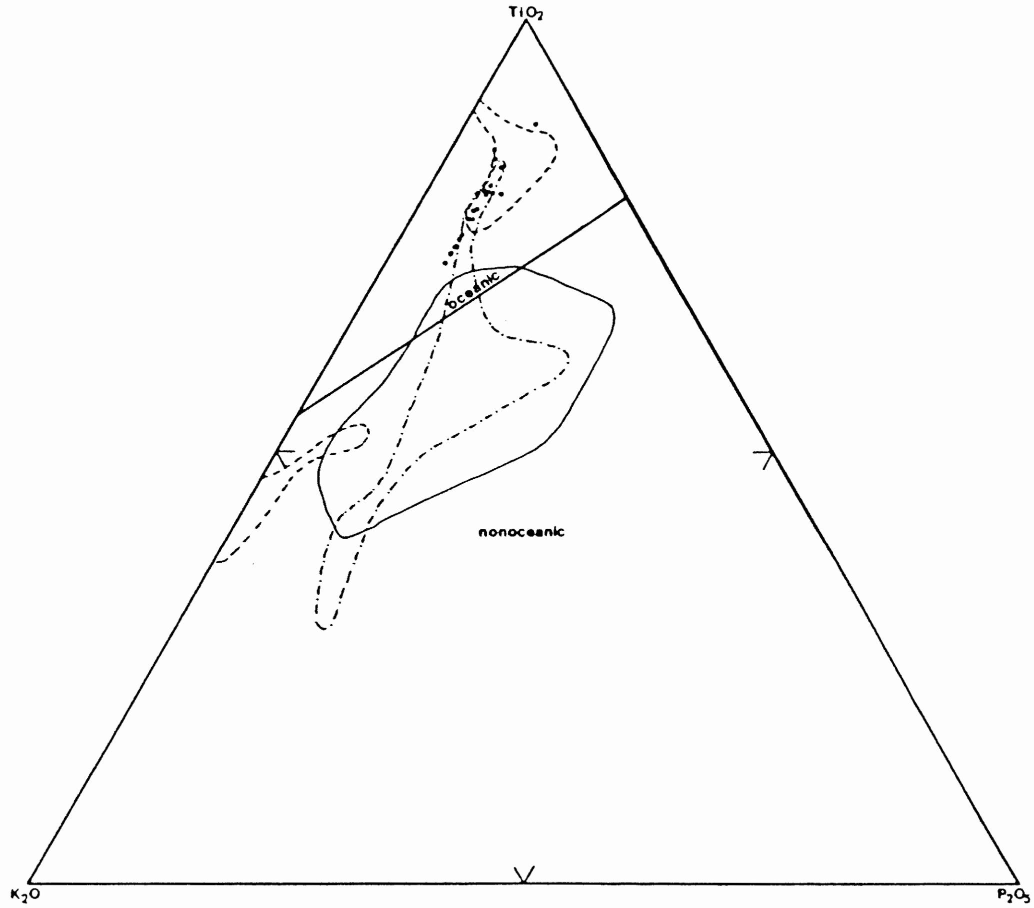

Figure 5.1 Plot of TiO2-K2O-P2O5. Circles indicate the pillow lava compositions for this study, dashed lines enclose the Crowdis Mountain samples, the solid field includes the Money Point samples, and the dash-dot line surrounds the Mabou Highlands samples. These three fields will be discussed in section 5.4. The oceanic and nonoceanic fields were defined by Pearce _et al_. (1974).

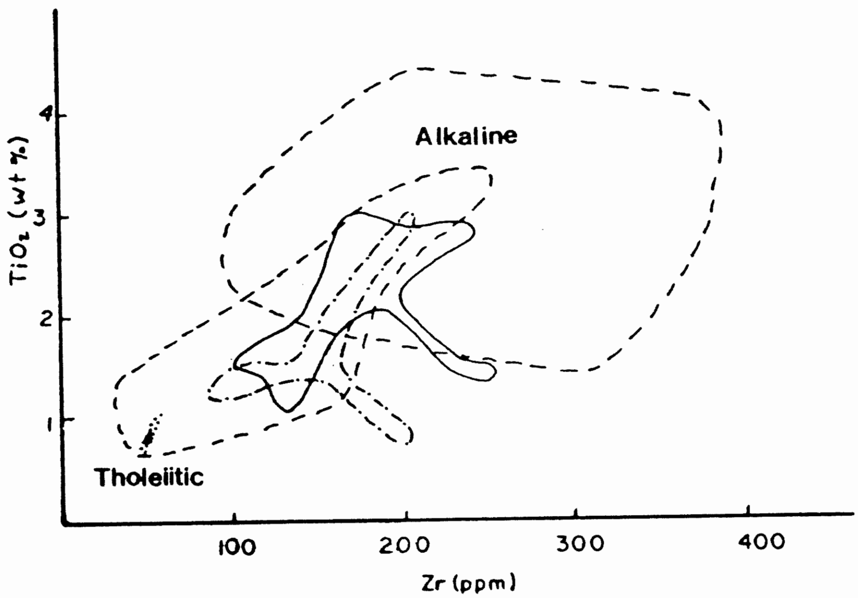

Figure 5.2 Plot of TiO_2 (wt %) versus Zr (ppm). Dashed lines indicate the alkaline and tholeiitic basalt fields defined by Floyd and Winchester (1976). Other fields are as described in figure 5.1.

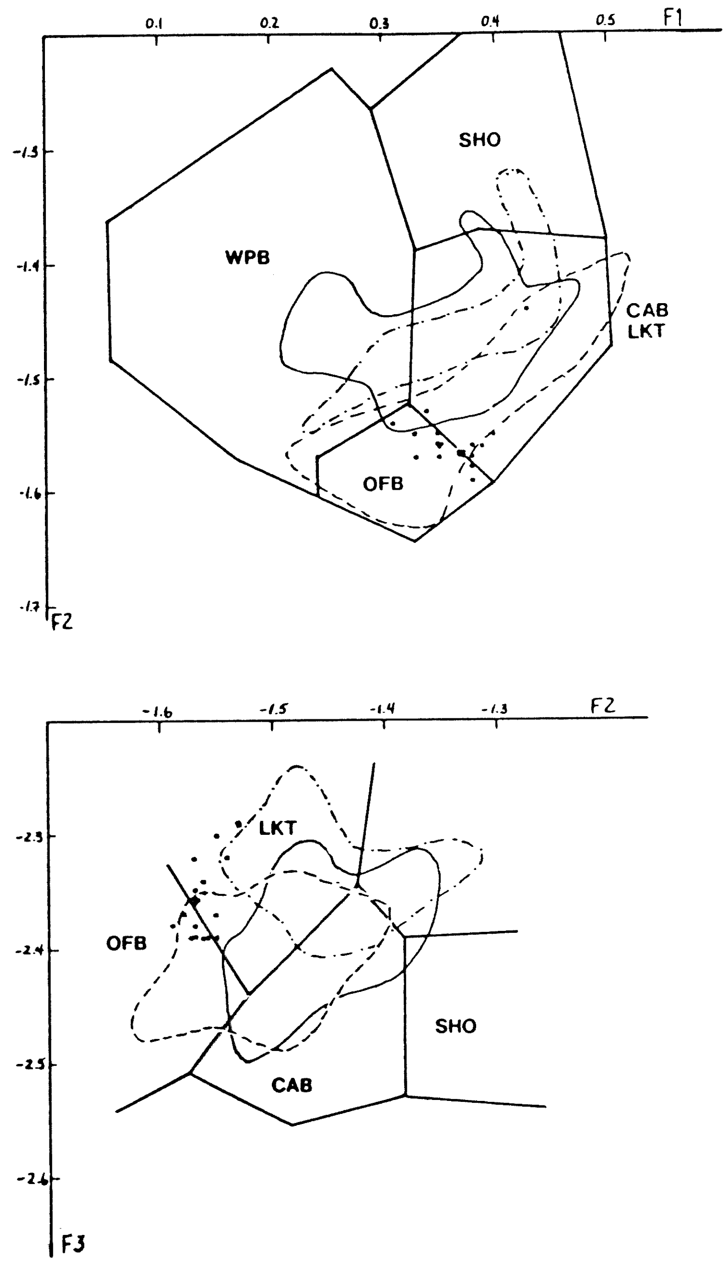

Figure 5.3 Plot of discriminant functions. The tectonic fields and calculation of the functions are taken from Pearce (1976). Samples from the other three locations are indicated as described in figure 5.1.

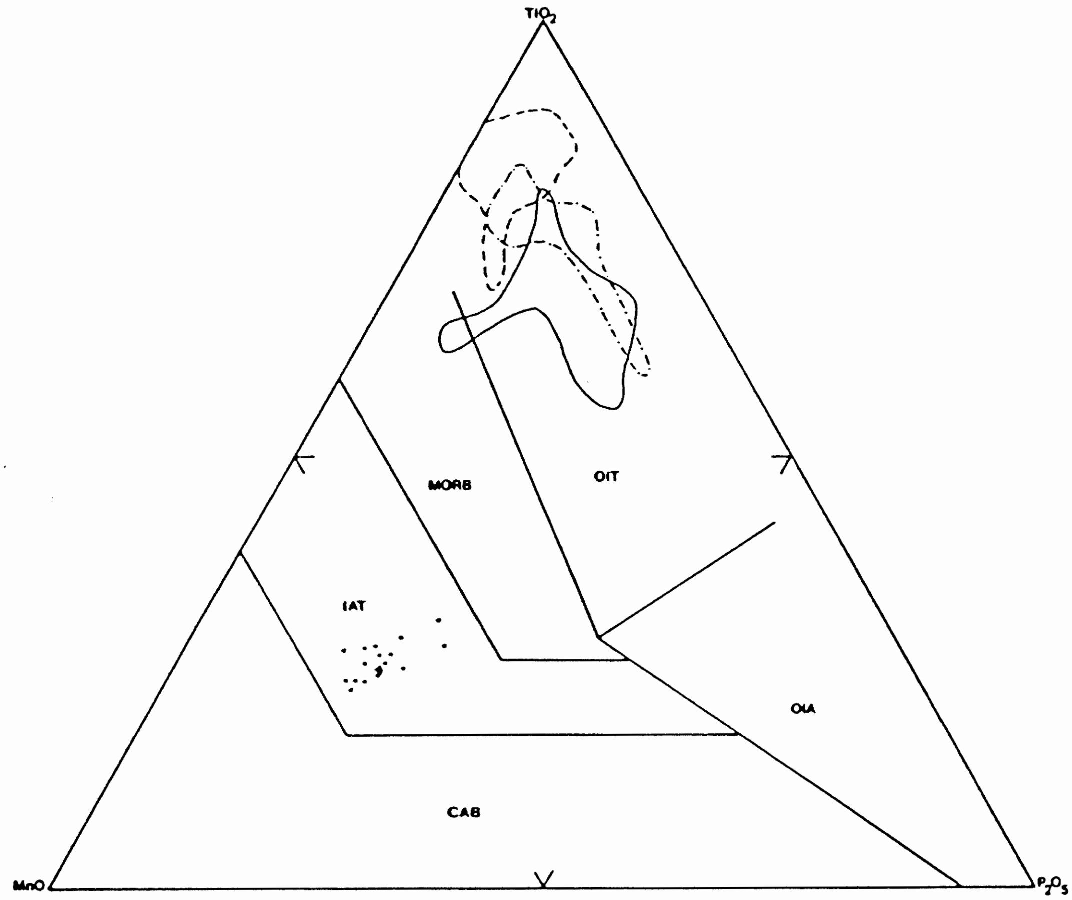

Figure 5.4 Plot of TiO2-MnO-P2O5. The tectonic fields were defined by Mullen (1983). Samples from the other three locations are indicated as described in figure 5.1.

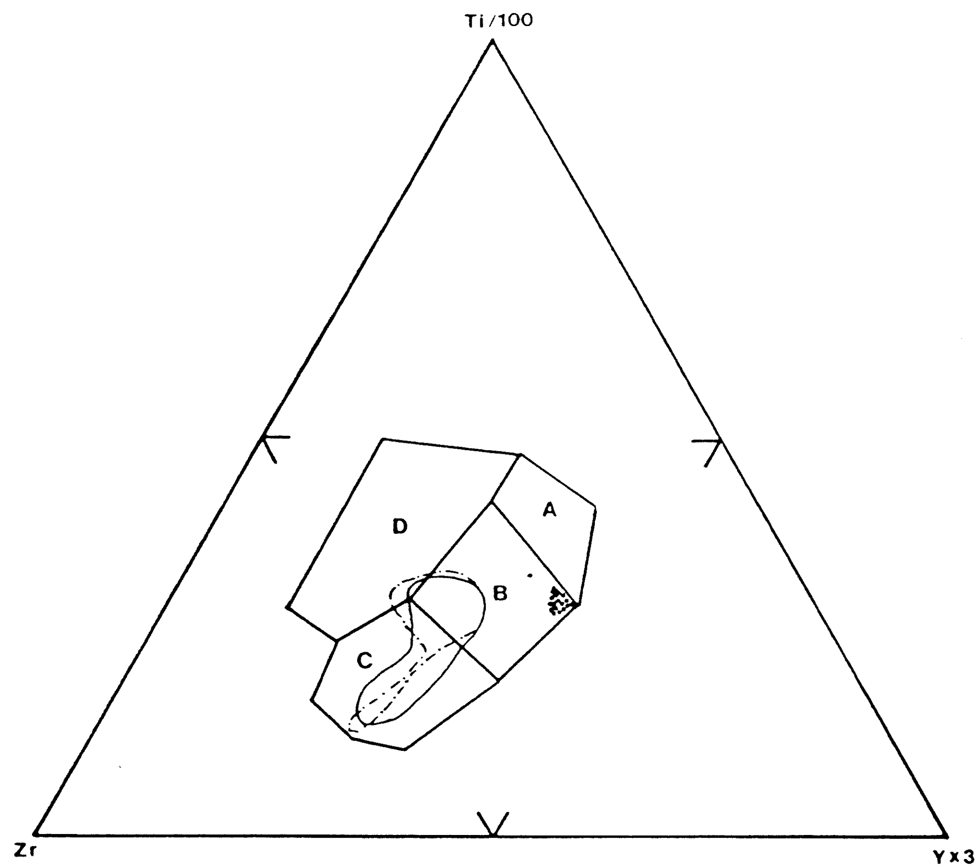

Figure 5.5 Plot of Ti-Zr-Y. Low potassium tholeiites plot in fields A and B, calc-alkaline basalts in fields C and B, ocean floor basalts in field B, and within plate basalts in field D. The tectonic fields were defined by Pearce and Cann (1973). Samples from Money Point and Mabou are indicated by the solid and dash-dot lines, respectively.

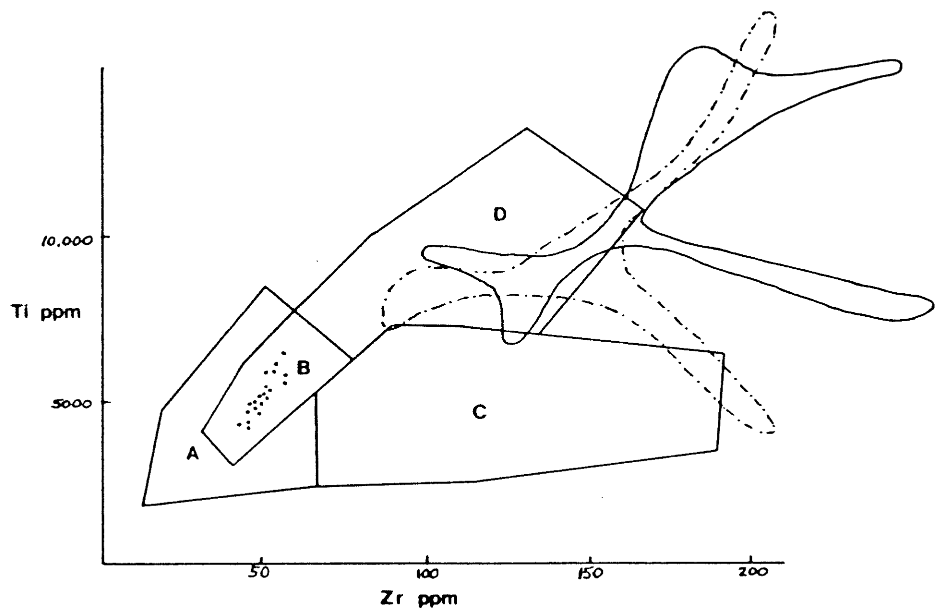

Figure 5.6 Plot of Ti (ppm) versus Zr (ppm) after Pearce and Cann (1973). Fields A, B, C, and D are the same as for figure 5.5. The Money Point and Mabou samples are indicated by the solid and dash-dot lines, respectively.

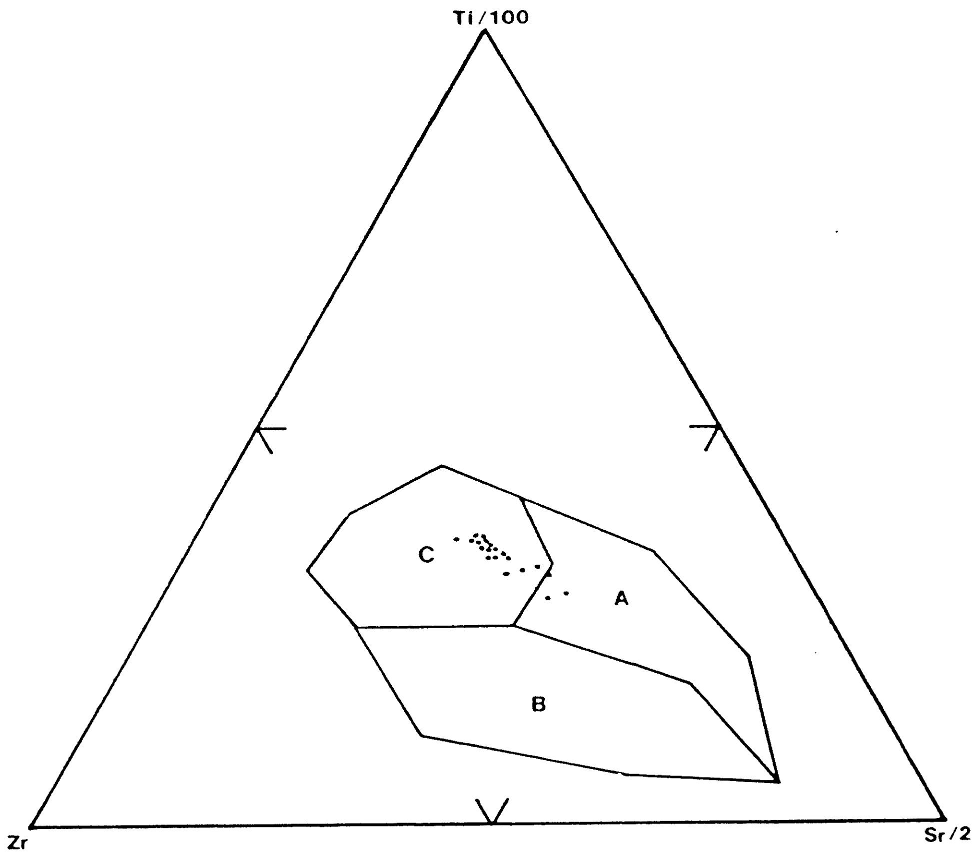

Figure 5.7 Plot of Ti-Zr-Sr. Low potassium tholeiites plot in field A, calc-alkaline basalts in field B, and ocean floor basalts in field C as defined by Pearce and Cann (1973).

another plot which was proposed by Pearce and Cann (1973). In figure 5.5, the samples plot in a tight cluster in field B along the boundary of field A. Next the authors recommend plotting the samples on a Ti-Zr-Sr diagram if the rocks are relatively fresh or plotting Ti versus Zr if the rocks are altered or metamorphosed. The pillow basalts have been metamorphosed to upper greenschist or lower amphibolite facies, therefore the Ti versus Zr diagram is appropriate. Once again the samples lie within field B (figure 5.6). The Ti-Zr-Sr diagram was also plotted to determine the relative mobility or enrichment of Sr. In this case the samples plotted within the ocean floor basalt and low potassium tholeiite fields (figure 5.7). The scatter of the points results largely from the variation in Sr, probably due to the presence of carbonate filled cavities in the pillow basalts.

5.3 COMPARISONS

Volcanic - sedimentary sequences of the Money Point Formation at Cape North, the Crowdis Mountain volcanics at Middle River, and within the Mabou Highlands are considered to be part of the western Highlands volcanic sedimentary complex. Geochemical analyses were obtained from Barr (pers comm. 1986) for the Money Point units, from Barr and MacDonald (in prep.) for the Mabou sequence, and from

Doucet (1983) for the Crowdis Mountain volcanic rocks. In comparison, the mafic volcanic rocks of Crowdis Mountain, Money Point, and Mabou show a wider range of values for most oxides. Trace element concentrations are available for Money Point and Mabou, but not for the Crowdis Mountain units. The wider range of values for all these units is clearly shown on the discriminant diagrams. In figure 5.1 most of the Middle River samples lie within the oceanic field, however the points do not show a roughly linear trend as the Faribault Brook pillow basalts do. Both the Mabou and Money Point samples show even more scatter with most of the points lying within the nonoceanic field. This may be due to a greater mobility of potassium in these rocks.

In the TiO2 versus Zr plot (figure 5.2) the Money Point and Mabou mafic metavolcanic rocks lie in both the alkaline and tholeiitic fields. These units have larger (and more variable) concentrations of both TiO2 and Zr.

The plot of discriminant functions (figure 5.3) shows more scatter for the Crowdis Mountain units, however most points plot in the same fields as the pillow basalts. The Money Point and Mabou Highland samples plot largely in the within plate and calc-alkaline/low potassium fields. Thus, some points lie in the same field as the pillow lavas, however the range of compositions is much greater. A fair degree of scatter is also evident in the TiO2-P2O5-MnO plot. The samples lie near the TiO2 apex for the other three units, possibly within the seamount tholeiite field. None of the samples plot in the vicinity of the pillow basalts.

The Ti-Zr-Y plot shows a distinct difference in composition between the Money Point and Mabou mafic volcanic units, which are similar, and the Faribault Brook pillow basalts. The pillow lavas again show a more restricted range of compositions. In the Ti versus Zr diagram of figure 5.6, the Money Point and Mabou units plot within field D (ocean floor basalt field) or outside the defined fields.

Aside from the differences shown in the discriminant diagrams, the Money Point and Mabou Highlands mafic metavolcanic layers have much lower levels of Ni and Cr and much higher levels of incompatible elements (ie. K2O, Rb, Ba, Zr, and Nb) in comparison to the pillow basalts.

5.5 DISCUSSION

Results of the discriminant diagrams must be interpreted with caution owing to the metamorphism of the pillowed sequence. However, most plots show a correlation between geochemically coherent elements, thus suggesting that mobilization of many elements (eg. Ti, Zr, Y, P) during metamorphism has not been significant. From the diagrams, it can be safely concluded that the basalts are tholeiitic and formed in an oceanic environment. The samples cluster in or near the low potassium tholeiite or island arc tholeiite field of several diagrams (low K tholeiites indicate an island arc setting). Taking the field observations into consideration, the island arc setting is a likely location for formation of a sequence of pillow basalts which are overlain by sediments with interbedded rhyolitic layers near the base. The samples also plot in the ocean floor basalt field of several diagrams. However, the association of felsic volcanic layers with the mafic volcanic rocks favors the island arc setting.

The mafic volcanic sequences of Money Point, Mabou, and Crowdis Mountain all show a wider range of compositions than the pillow lavas. This may be a result of greater mobility of elements during metamorphism or indicate the presence of different units within these sequences. It should be noted that the pillow basalts are the best preserved unit, therefore suggesting that this unit has not undergone the same degree of remobilization.

The Crowdis Mountain volcanic samples show the most overlap with the pillow basalts on the major and minor oxide diagrams, but unfortunately trace element concentrations are not available at this time. The Money Point and Mabou units appear to have compositions which are distinct from the pillow basalts of the Faribault Brook area. The tholeiitic pillow basalts are rich in compatible elements such as Ni and Cr and contain very low levels of incompatible elements, while the Money Point and Mabou mafic volcanic rocks contain low levels of compatible elements and much higher levels of incompatible elements. This suggests that the tholeiitic Faribault Brook basalts may represent less evolved material, while the alkaline Money Point and Mabou units represent more evolved basalts.

CHAPTER SIX

ECONOMIC GEOLOGY

6.1 INTRODUCTION

Opaque minerals are found throughout both the metasedimentary and metavolcanic units. Pyrite, arsenopyrite, galena, sphalerite, chalcopyrite, and pyrrhotite are found as tiny stringers, disseminated on foliation surfaces, concentrated in small fractures, or disseminated throughout the samples. The major concentrations of sulphide minerals are associated with the quartz sericite schist or low angle ductile shear zones. In outcrop no evidence of shearing is visible in the mineralized sericite schists, but slabbed samples show folding and possibly shearing.

The economic importance of the quartz sericite schist is also emphasized by Covey (1979). He states that the quartz sericite schist is almost always the host rock of the sulphide mineralization and cites several examples which were noted in drill core or outside the study area of this project.

The principal zones of mineralization occur at three old prospects, Galena Mine, Core Shack, and Silver Cliff (figure 1.2), and in a relatively flat lying shear zone within the pillow lava sequence (from X to Y, figure 1.2). All deposits are stratabound. At Galena Mine and Core Shack the mineralization is associated with the quartz sericite schist, while the host at Silver Cliff is somewhat different in composition.

6.2 MINOR OCCURRENCES

Slightly elongate grains of ilmenite and anatase-rutile comprise 1 to 3 percent of the pelitic layers (figure 6.1). Ilmenite also occurs as lamellae along the cleavage planes in biotite. The oxides show consistent alignment parallel to the foliation and crenulation.

The semipelitic layers contain up to 10 or 15 percent opaque minerals, which include galena, arsenopyrite, chalcopyrite, pyrrhotite, sphalerite, ilmenite, and anatase-rutile. In one sample galena shows distinct elongation parallel to the foliation (figure 6.2) and the arsenopyrite has fractured perpendicular to the flattening direction. Ilmenite and quartz form inclusion trails in garnet which overgrows the matrix crenulation. Locally, the sulphide minerals appear to be replacing quartz augen or vein quartz.

In psammitic zones the opaque minerals occur as irregular blebs or slightly elongate grains which trend parallel to the foliation and comprise between 1 and 3

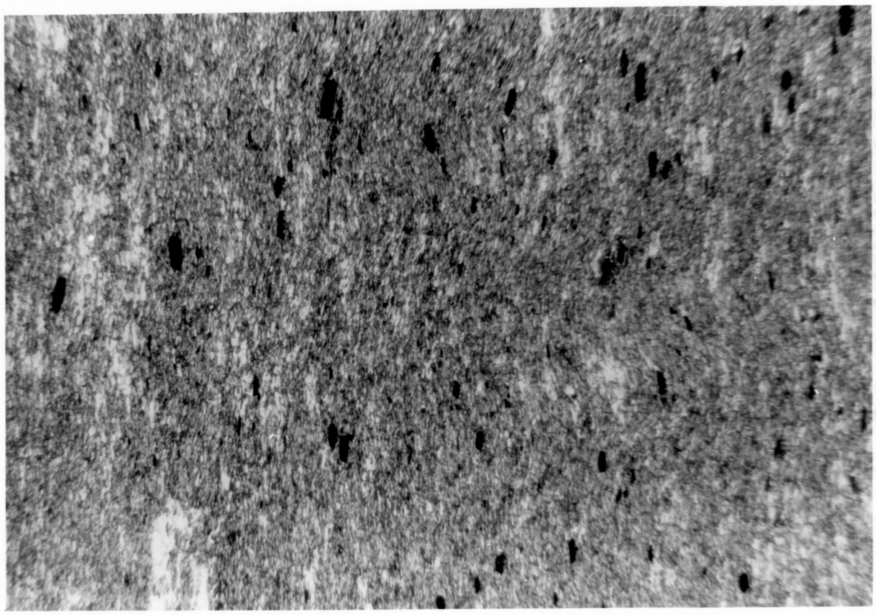

Figure 6.1 Elongate grains of ilmenite and anatase - rutile are consistently aligned parallel to the foliation (S1) and the crenulation (S2) in the pelitic layers. The field of view is 5*3.4 mm.

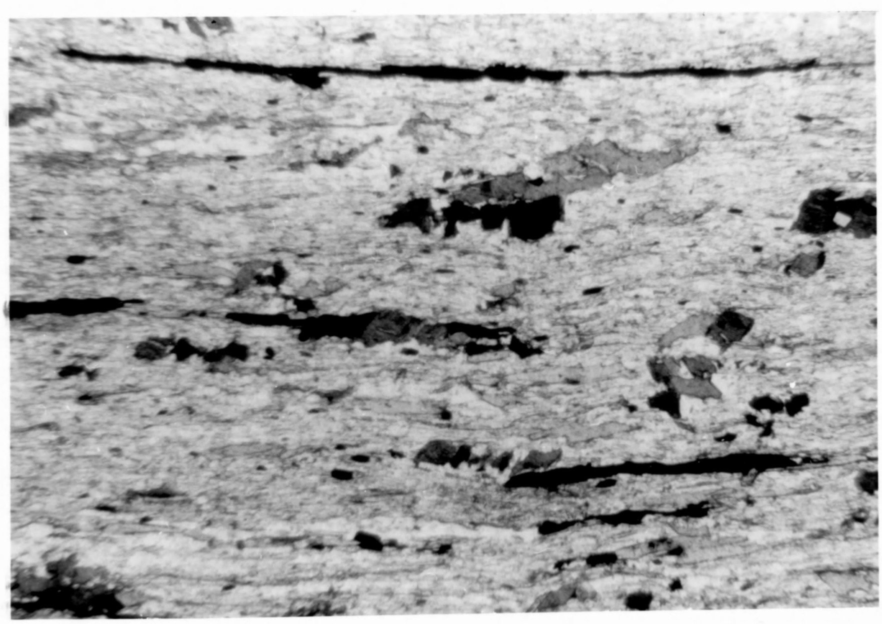

Figure 6.2 Very elongate grains of galena are stretched parallel to the foliation in the semipelites.

percent of the sample. Galena, ilmenite, and anatase-rutile have been identified.

The pillow basalts typically contain less than 1 or 2 percent opaque grains. However, the dioritic layers contain up to 15 or 20 percent opaque minerals which are aligned parallel to the hornblende crystals. Arsenopyrite and ilmenite show intergrowth with the hornblende (figure 4.5). Colloform sphalerite and pyrite are associated with the arsenopyrite. Galena shows a distinct sieve texture along grain edges and is also associated with the sphalerite.

6.3 GALENA MINE

At the Galena Mine prospect four adits and the rusted machinery of a concentrating plant remain from the mining operations of the late 1800's and early 1900's. The sulphides are found near the top of a 3 to 4 metre thick quartz sericite schist layer within a zone of interlayered pelites, semipelites, and psammites. The massive sulphides, chiefly galena, sphalerite, and arsenopyrite with minor chalcopyrite and/or pyrrhotite, occur in lenses, but overall the deposit appears stratiform. The hand specimen shows folding and possibly shearing in the mineralized zone (figure 6.3).

A polished thin section from the sulphide rich zone reveals an intergrowth of galena and sphalerite. Inclusions of chalcopyrite and possibly pyrrhotite are present in the sphalerite. Locally, well formed crystals of galena are present, but most sulphides form irregular grains. The arsenopyrite shows fracturing, brecciation and recrystallization (figure 6.4). Chatterjee (1980) reports rare stibnite and bismuthinite.

6.4 CORE SHACK

One of the exploration companies cleared the Core Shack showing with a bulldozer, leaving good exposure of the mineralized zone, which is truncated by an east-west fault at the north end of the property. The sulphides are concentrated in layers within a 5-6 metre thick unit of the quartz sericite schist. The mineralized horizon of quartz sericite schist has been correlated between Galena Mine and Core Shack using drill hole data from various companies (Covey, 1980).

Sphalerite, arsenopyrite, galena, and pyrite are visible in hand specimens. Chatterjee (1980) also reports pyrrhotite, argentite, and chalcopyrite at this location. The mineralized zone is noted by the yellow to rust color and the soft, crumbly nature of the outer weathered layer. Arsenopyrite comprises over 95 percent of the sulphides from one mineralized layer. Minor pyrite and/or pyrrhotite are associated with the arsenic sulphide. The arsenopyrite commonly occurs as irregular grains with a large variation in grain size. Both recrystallization and later (?) brittle deformation are evident. Locally, rhombic crystals are observed.

Sulphide minerals are also observed to replace quartz augen in relatively less mineralized layers of the quartz sericite schist. In thin section, the less mineralized zones contain galena which lies within the foliation plane (figure 6.5). Sphalerite and chalcopyrite are associated with the galena and commonly fill cracks in the mineral. Brittle deformation is evident.

6.5 SILVER CLIFF

At present, the mineralized zone at Silver Cliff is poorly exposed and covered by debris. Chaterjee (1980) described a zone of mineralization which was exposed over 45 metres and varied from 2 to 8 metres in width, with the sulphides present in concordant to discordant folded lenses.

The dominant lithology is a chlorite rich schist, probably volcanic in origin, which locally contains random or parallel hornblende and/or biotite porphyroblasts. The mineralization is closely associated with a massive, sugary textured quartz-carbonate unit. A garnetiferous, sulphide bearing unit, which was described by Chatterjee (1980), was found mainly as boulders, but a small, deformed outcrop was uncovered and the garnetiferous rock appeared to be associated with the quartz - carbonate unit.

Figure 6.3 A sample of the quartz sericite schist from Galena Mine showing deformation of the mineralized zones. The quartz sericite schist at the base of the sample may be sheared, while folding of a quartz sericite lens is visible on the side of the sample. The dark layer consists largely of galena, sphalerite, arsenopyrite, and quartz. The white square is 1*1 cm.

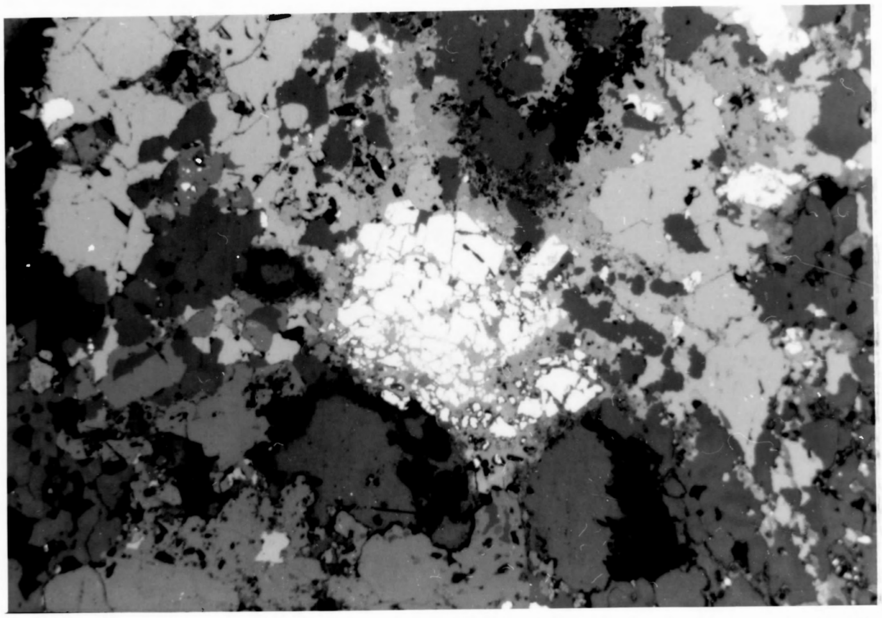

Figure 6.4 Brecciation of arsenopyrite in the Galena Mine mineralized zone indicating brittle deformation. The field of view is .5*.34 mm.

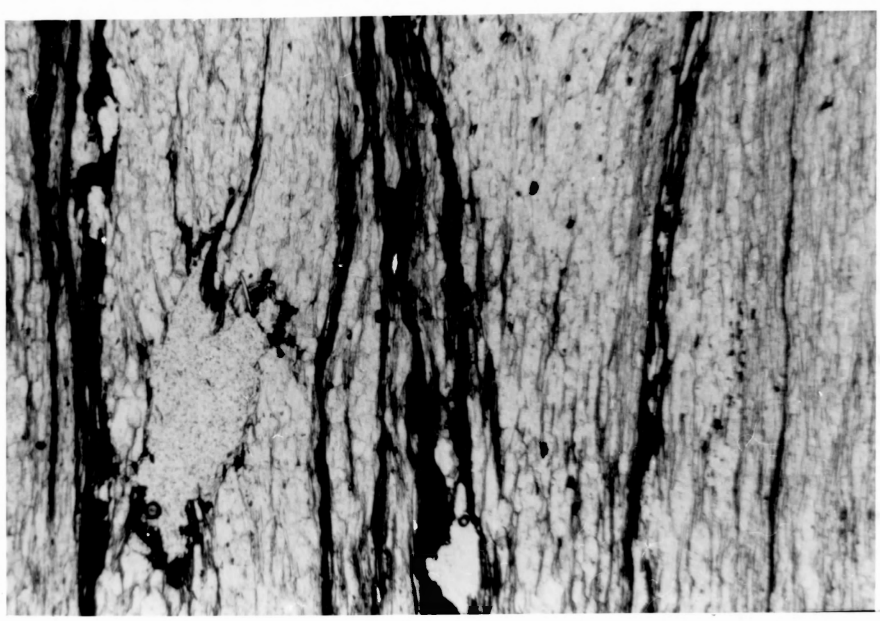

Figure 6.5 Galena parallel to the foliation plane in the quartz sericite schist. The field of view is 5*3.4 mm.

Sphalerite, arsenopyrite, galena, pyrite, and pyrrhotite were noted in outcrop. A polished section from the mineralized zone at Silver Cliff reveals an assemblage of arsenopyrite, galena, sphalerite, chalcopyrite, and pyrrhotite. The recrystallized grains of arsenopyrite are commonly intergrown with chalcopyrite and sphalerite. The arsenopyrite occurs as irregular grains or, rarely, as rhombic crystals. The sphalerite contains chalcopyrite inclusions. Grains of galena range from idiomorphic to irregular. Chatterjee (1980) also identified pyrite, tetrahedrite, argentite, bismuthinite, and lollingite.

Inadequate exposure prevents a thorough comparison of Silver Cliff with Galena Mine and Core Shack. The presence of the volcanic (?) chlorite schist indicates a possible difference in the host rock. However, petrographic studies indicate that the mineralized zones have similar mineral asseblages (Appendix A - samples 18, 21ee, and 28).

6.6 MINERALIZED SHEAR ZONES

The mineralized shear zones preferentially occur in the incompetent schistose layers within the pillow sequence. Sulphides such as arsenopyrite, pyrite, galena, sphalerite, and minor chalcopyrite are present. At one location large grains of arsenopyrite (1 centimetre in diameter) dominate the assemblage. In thin section, the arsenopyrite shows intense brecciation, along with metamorphic recrystallization. Slightly colloform sphalerite surrounds and fills cracks in the arsenopyrite. Chalcopyrite is present as inclusions in the sphalerite or as a separate phase associated with arsenopyrite. A manganese (?) oxide or hydroxide, possibly pyrolusite or manganite, is present as an alteration product. It is associated with the arsenopyrite and sphalerite (figure 6.6).

Another polished thin section of the mineralized shear zone shows pyrrhotite being replaced by colloform hematite (figure 6.7). Chalcopyrite and galena are both associated with the pyrrhotite. Sieve textured needles of ilmenite and anatase-rutile are present.

6.7 DISCUSSION

Observations of hand samples and thin sections indicate the presence of the sulphides (and oxides) prior to the deformation. The sample from Galena Mine (figure 6.3) shows folding and shearing of the host and massive sulphides. Several thin sections and polished sections contain both sulphides and oxides which are oriented parallel to the foliation. In some cases, the sulphides are distinctly drawn out in the plane of flattening, while more competent grains show fracturing perpendicular to the plane of flattening. Metamorphic recrystallization is most prominent in the arsenopyrite due to the strong anisotropy of this

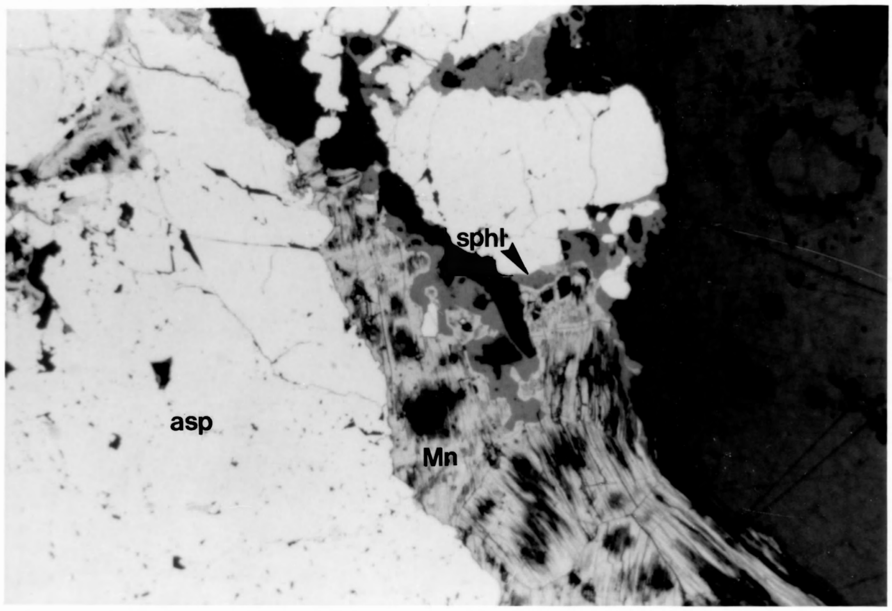

Figure 6.6 A Mn (?) oxide or hydroxide in a sample from a ductile shear zone. The Mn mineral is an alteration product and is associated with both arsenopyrite and sphalerite. The field of view is .5*.34 mm.

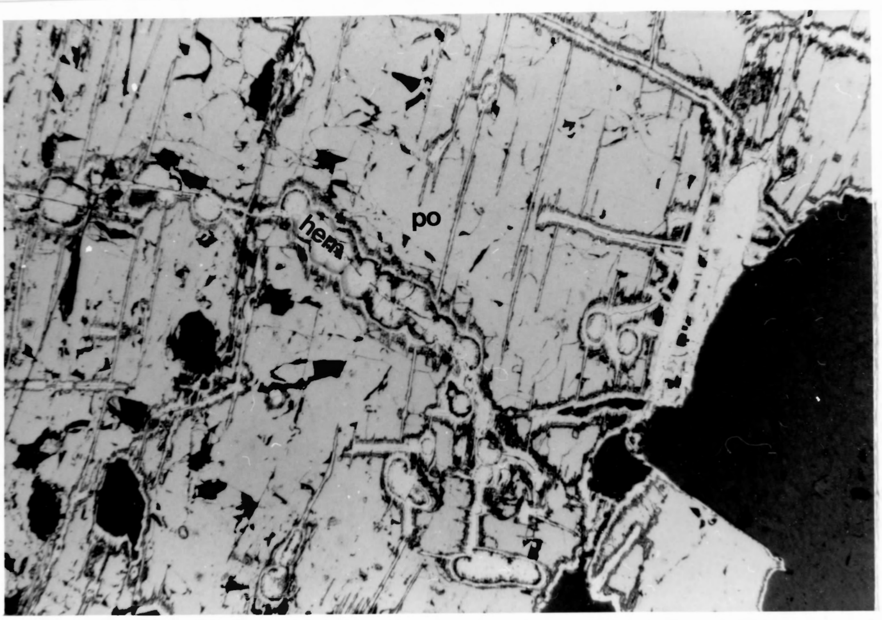

Figure 6.7 Replacement of pyrrhotite by colloform hematite. The field of view is .5*.34 mm.

mineral. Refer to figure 4.7 for a summary of the sulphide deposition and deformation with respect to the metamorphism and deformation of the host rock.

The most common sulphides recognized in the highly mineralized areas are galena, arsenopyrite, sphalerite, chalcopyrite, and pyrrhotite, +/- pyrite. Therefore, the chief metals present are Cu, Pb, Zn, Fe and As. The presence of arsenopyrite suggests that this may have been a favorable environment for the deposition of gold. Assayed samples generally contain trace amounts of Au and Ag (Covey, 1979). Chatterjee (1980) reports a very strong positive correlation in a scatter diagram of oz per ton of gold versus weight percent of arsenic.

Regardless of the fact that the Cu sulphides occur only as minor phases, the association of base metals with a felsic volcanic host leads to interesting possibilities for the origin of the sulphides. The observation that the sulphide minerals were present prior to deformation and the association of base metals with the felsic volcanic layers favors the possibility of a syngenetic origin.

Shear zones have aided in remobilization of the sulphide minerals. Quartz and arsenopyrite within the main shear zone show metamorphic recrystallization. Brittle deformation of the sulphides is evident as well, both in the shear zones and in thin sections of the mineralized quartz sericite schist.

Chatterjee (1980) plots metal abundances of Cu, Pb, Zn, Au, and Ag from the Faribault Brook area, in order to compare with distributions for known concordant and hydrothermal discordant ore bodies. He concluded that the relative abundance of Cu, Pb, and Zn is not similar to that shown by concordant ore bodies and more closely resembles the abundances for the Conrad hydrothermal discordant ore body of Australia.

However, the sulphides have undergone remobilization during metamorphism and deformation. Therefore, the relative abundance of Cu, Pb, and Zn in any assay will not be equivalent to the original values. Differences in ease and degree of remobilization for the sulphide minerals or PT conditions and fluid compositions during metamorphism and deformation which differ from original conditions during deposition will result in new relative abundances between the Cu, Pb, and Zn phases after deformation. Therefore, any relative abundance patterns are unreliable as an indicator of the original nature of the deposit.

CHAPTER SEVEN

DISCUSSION AND CONCLUSIONS

7.1 DISCUSSION AND CONCLUSIONS

The deformation and metamorphic recrystallization of the sulphide phases indicates that the sulphide minerals were present before the deformation occurred. It has been determined, from the metamorphic assemblages, that the complex has undergone upper greenschist to lower amphibolite facies grade metamorphism. The metamorphic textures indicate that metamorphism began during the development of the pervasive foliation and peaked late in the deformation during or after the development of the crenulation.

Three stages of deformation were discussed in section 3.10. The development of the foliation was placed in D1 and the crenulation in D2 with coaxial structures. However, evidence from metamorphic textures suggests that progressive metamorphism began during D1 and continued well into D2 (figure 4.7). Therefore, it is probable that D1 and D2 represent a continuous period of deformation during which orientation of the stress field changed.

The association of the sulphides with the quartz sericite schist was recognized early in the study. However, petrographic studies were completed before direct evidence of the volcanic nature of the schist was obtained. The significance of this association was discussed in section 6.7. Concentrations of sulphide minerals are also associated with ductile shear zones. The presence of significant mineralization in the shear zones suggests remobilization of the sulphides during deformation.

Mineralized zones in the Faribault Brook area have often been described as irregular and lenticular in assessment reports by various exploration companies. The lenticular nature may be due to a stretching of the mineralized layers parallel to the prominent elongation direction. It was noted in chapter three that the lineations, crenulations, upright folds, and the long axes of the pillows were all aligned north-south. Therefore it is probable that the orientation and shape of the mineralized layers have also been modified into north - south trending elongate masses during the deformation. Complete remobilization due to shearing has also affected the present distribution of the sulphide minerals.

If the complex did form in an island arc setting, as proposed in section 5.5, then the association of base metals with felsic volcanic rocks suggests a volcanogenic exhalative origin for the mineralization. The mineralization occurs in largely conformable felsic volcanic layers just above the volcanic - sedimentary interface as is expected in volcanogenic exhalative deposits. Common associations in these type of deposits include pyrite, pyrrhotite, sphalerite, galena, chalcopyrite, arsenopyrite, magnetite, and tetrahedrite (Evans, 1980). Magnetite and tetrahedrite were not noted in this study, but Chatterjee (1980) reported both. Evans (1980) also suggests that Au and Ag are commonly present in volcanogenic exhalative deposits.

A similar, but larger scale, occurrence of base metal mineralization is found at the Brunswick 12 and 6 localities in northern New Brunswick. The following description is taken from van Staal and Williams (1984). The host rock consists of fine to coarse grained metasediments, felsic and mafic metavolcanic units, which include pillowed flows, agglomerates, and tuffs. The probable age of the sequence is Ordovician with sedimentation beginning as early as the Cambrian. The base metal sulphides are associated with the felsic volcanic units and occur in three zones of differing sulphide mineralogy. A unit of banded iron formation occurs with the sulphides.

The polyphase deformation history closely resembles that of the Faribault Brook area. Two periods of isoclinal folding (mm to km scale) produced transposition of the original layering and an axial plane foliation which is parallel to the transposed layering. Macroscopic shear zones are parallel to the foliation and are overprinted by upright, open to tight folds of the third deformation period. An axial planar crenulation cleavage and parallel lineations developed with these folds. The last two stages of deformation produced kink bands (mm to cm scale) with fractures along the steeply dipping axial planes and steep faults which trend between north and west.

Some differences arise between the types and amount of sulphides present. The Brunswick 12 and 6 mines have more pyrite associated with the deposits and arsenopyrite is not present. The occurrence of banded iron formation is lacking in the Faribault Brook area. However, the overall lithologies are comparable and the two areas appear to have undergone a very similar history of deformation.

CHAPTER EIGHT

IMPLICATIONS AND RECOMMENDATIONS

The recognition that the sulphide minerals are associated with the felsic volcanic layers of a volcanic - sedimentary sequence provides a target for further economic exploration. Other exposures of the western Highlands volcanic sedimentary complex should be examined with this association in mind. The stratigraphic control on mineralization makes the possibility of repetition through folding very important. Repetition of distinct horizons was not noted during this study, however a more detailed analysis of the structure may yield better evidence.

The identification of the pillow lavas and the felsic volcanic units leads to implications concerning the tectonic setting of this sequence. Further comparison of geochemical data with other mafic volcanic sequences in Cape Breton and surrounding regions (ie. New Brunswick and Newfoundland) is suggested. Additional sampling of the quartz sericite schist for geochemical analysis is recommended. Determination of the composition of this felsic volcanic unit may lead to further constraints on the origin of the sequence and the associated sulphide minerals. Comparison of other acid volcanic rocks within the western Highlands volcanic sedimentary complex should also be made.

Due to time contraints no microprobe analysis was done for this study. A polished section is available for analysis of coexisting biotite and garnet to better constrain the conditions of metamorphism. Accurate identification of some sulphide minerals, such as the possible Mn oxide or hydroxide, can also be made by microprobe analysis. Geothermometers and geobarometers involving sulphide minerals may be applicable.

REFERENCES

Barr, S.M., Jamieson, R.A., and Raeside, R.P., 1985, Igneous and metamorphic geology of the Cape Breton Highlands; GAC/MAC 1985 Excursion 10 Guidebook, 48p.

Barr, S.M. and MacDonald, A.S., in prep., Geology of the Mabou Highlands; Nova Scotia Department of Mines and Energy Paper.

Barr, S.M., MacDonald, A.S., Blenkinsop, J., and Pride, C.R., in press, The Cheticamp pluton: a peraluminous granitoid intrusion in the western Cape Breton Highlands, Nova Scotia; Canadian Journal of Earth Sciences.

Bell, T., 1985, Deformation partitioning and porphyroblast rotation in metamorphic rocks: a radical re-interpretation; Journal of Metamorphic Geology, 3, pp. 109-118.

Bickle, M.J. and Archibald, N.J., 1984, Chloritoid and staurolite stability: implications for metamorphism in the Archean Yilgarn Block, W.A.; Journal of Metamorphic Geology, 2, pp. 179-203.

Chatterjee, A.K., 1980, Mineralization and associated wall rock alteration in the George River Group, Cape Breton

Island, Nova Scotia; Unpublished Ph.D. thesis, Dalhousie University, 197p.

Conrod, D.M., 1984, The relationship between low and high grade metamorphic rocks in the French Mountain area, Cape Breton Highlands, Nova Scotia; Unpublished B.Sc. thesis, Dalhousie University, 209p.

Cormier, R.F., 1972, Radiometric ages of granitic rocks, Cape Breton Island, Nova Scotia; Canadian Journal of Earth Sciences, 9, pp. 1074-1086.

Covey, G., 1979, Nova Scotia Department of Mines and Energy Assessment File 11K/10B, 7-J-09(48).

Covey, G., 1980, Nova Scotia Department of Mines and Energy Assessment File 11K/10B, 7-J-09(49).

Craw, D., 1984, Tectonic stacking of metamorphic zones in the Cheticamp River area, Cape Breton Highlands, Nova Scotia; Canadian Journal of Earth Sciences, 21, pp. 1229-1244.

Currie, K.L., in press, Relations between magmatism and metamorphism near Cheticamp, Cape Breton Island, Geological Survey of Canada Bulletin.

Currie, K.L., 1982, Paleozoic supracrustal rocks near Cheticamp, Nova Scotia; Maritime Sediments and Atlantic Geology, 18, pp. 94-103.

Currie, K.L., Loveridge, W.D., and Sullivan, R.W., 1982, A U-Pb age on zircon from dykes feeding basal rhyolitic flows of the Jumping Brook Complex, northwestern Cape Breton Island, Nova Scotia; Current Research, Part C, Geological Survey of Canada Paper 82-1C, pp. 125-128.

Davis, G.H., 1984, Structural Geology of Rocks and Regions; John Wiley and Sons, New York, 492p.

Doucet, P., 1983, The petrology and geochemistry of the Middle River area, Cape Breton Island, Nova Scotia; Unpublished M.Sc. thesis, Dalhousie University, 339p.

Evans, A.M., 1980, An Introduction to Ore Geology; Elsevier Scientific Publishing Co., New York, 231p.

Floyd, P.A. and Winchester, J.A., 1975, Magma type and tectonic setting discrimination using immobile elements; Earth and Planetray Science Letters, 27, pp. 211-218.

Holdaway, M.J., 1971, Stability of andalusite and the aluminum silicate phase diagram; American Journal of Science, 271, pp. 97-131.

Hoschek, G., 1969, The stability of staurolite and chloritoid and their significance in the metamorphism of pelitic rocks; Contributions to Mineralogy and Petrology, 22, pp. 208-232.

Jamieson, R.A., van Breeman, O., Sullivan, R.W., and Currie, K.L., in press, The age of igneous and metamorphic events in the western Cape Breton Highlands, Nova Scotia; Canadian Journal of Earth Sciences.

Jamieson, R.A. and Craw, D., 1983, Reconnaissance mapping of the southern Cape Breton Highlands - a preliminary report; Current Research, Part A, Geological Survey of Canada Paper 83-1A, pp. 263-268.

Jamieson, R.A. and Doucet, P., 1983, The Middle River - Crowdis Mountain area, southern Cape Breton Highlands; Current Research, Part A, Geological Survey of Canada, Paper 83-1A, pp. 269-275.

Keppie, J.D. and Smith, P.K., 1978, Compilation of isotopic age data of Nova Scotia; Nova Scotia Department of Mines Report 78-4.

La Tour, T.E., Kerrich, R., Hodder, R.W., and Barnett, R.L., 1980, Chloritoid stability in very iron-rich pillow lavas; Contributions to Mineralogy and Petrology, 74, pp. 165-173.

MacDonald, A.S. and Smith, P.K., 1980, Geology of Cape North area, Northern Cape Breton Island, Nova Scotia; Nova Scotia Department of Mines and Energy, Paper 80-1, 60p.

Milligan, G.C., 1970, Geology of the George River Series, Cape Breton; Nova Scotia Department of Mines Memoir 7, 111p.

Mullen, E.D., 1983, MnO/TiO2/P2O5: a minor element discriminant for basaltic rocks of oceanic environments and its implications for petrogenesis; Earth and Planetary Science Letters, 62, pp. 53-62.

Neale, E.R.W. and Kennedy, M.J., 1975, Basement and cover rock at Cape Breton Island, Nova Scotia; Maritime Sediments and Atlantic Geology, 11, pp. 1-4.

Raeside, R.P., Barr, S.M., and Jong, W., 1984, Geology of the Ingonish River - Wreck Cove area, Cape Breton Island, Nova Scotia; Nova Scotia Department of Mines and Energy Report 84-1, pp. 249-258.

Pearce, J.A., 1976, Statistical analysis of major element patterns in basalts; Journal of Petrology, 17, pp. 15-43.

Pearce, J.A. and Cann, J.R., 1973, Tectonic setting of basic volcanic rocks determined using trace element analysis; Earth and Planetary Science Letters, 19, pp. 290-300.

Pearce, T.H., Gorman, B.E., and Birkett, T.C., 1975, The TiO2-K2O-P2O5 diagram: a method of discriminating between oceanic and non-oceanic basalts; Earth and Planetary Science Letters, 24, pp. 419-426.

Plint, H.A., Connors, K.A., and Jamieson, R.A., in prep, Geology and mineralization of the western highlands metavolcanic - metasedimentary complex, Cheticamp - Pleasant Bay area, Cape Breton Island; Current Research, Part C, Geological Survey of Canada.

Ponsford, M. and Lyttle, N.A., 1984, Metallic mineral occurrences map and data compilation, Eastern Nova Scotia; Nova Scotia Department of Mines and Energy Open File Report 600, 24p.

Turner, F.J., 1981, Metamorphic Petrology : Mineralogical, Field, and Tectonic Aspects, Hemisphere Publishing Corporation, Washington, D.C., 524p.

van Staal, C.R. and Williams, P.F., 1984, Structure , origin, and concentration of the Brunswick 12 and 6 ore bodies, Economic Geology, 79, pp. 1669-1692.

APPENDIX A

Petrographic Descriptions

Twenty-nine samples from the major units and mineralized zones are described. The sample locations are given on the sample location on page 101.

Mineral abundance values are only approximations. The plagioclase and quartz are too fine grained to separate in some of the mafic volcanic samples. Therefore, only a combined total is given in a few cases. The individual opaque minerals are listed for any sample for which a polished thin section was prepared. However, sulphide and oxide minerals are grouped together as opaques for other samples.

The mineral abbreviations are:

ms - muscovite
qz - quartz
gt - garnet
bt - biotite
op - opaques (oxides and sulphides)
tm - tourmaline
sph - sphene
chl - chlorite
chlt - chloritoid
ap - apatite
cb - carbonate
pl - plagioclase
Ksp - K-feldspar
fsp - feldspar (both pl and Ksp)
hb - hornblende
ep - epidote
asp - arsenopyrite
ilm - ilmenite
a-r - anatase-rutile
gal - galena
sphl - sphalerite
chal - chalcopyrite
po - pyrrhotite
py - pyrite
pyrl - pyrolusite
man - manganite
hem - hematite

Pelites

K21k	ms(70%), qz(20%), gt(5%), bt(2%), op(3%), minor tm & sph, retro. chl (op-asp,ilm)	pronounced fol(ms,qz) & cren, poik gt - qz incl trails overgrow matrix, bt random, op parallel fol, relict bedding at a high angle to fol
K43c	ms(70%), qz(25%), gt(1%), op(3%), minor tm & sph	pronounced fol(ms,qz) & cren, fractured subidio gt syn-post S2, op parallel fol, boudinaged qz vein
K45	ms(65%), qz(23%), gt(5%), chlt(2%), op(4%), minor tm & sph, (op-ilm,a-r)	pronounced fol(ms,qz) & cren, poik gt - incl trails(qz,op) overgrow matrix, idio chlt & op parallel to fol

Semipelites

KH9	ms(50%), qz(31%), gt(7%), bt(8%), op(<5%), minor tm sph & ap, retro chl (op-ilm,a-r)	pronounced fol(ms,qz,bt) & cren, layering (rel % ms & qz), random bt with alt to chl, poik gt - incl trails overgrow matrix, op random or parallel, S1 parallel to S0 & S2 at a high angle
K20b	(gt rich layer) gt(35%), bt(25%), qz(22%), chl(12%), op(2%), chlt(4%), minor tm & sph	no fol, fractured poik gt - qz inclusions
K20b	(chlt rich layer) ms(40%), qz(25%), chlt(20%), gt(5%), bt(5%), op(5%), minor tm & sph	vague fol, random poik chlt, late kinks (S3) cut chlt
K25c	qz(48%), ms(35%), bt(10%), pl(5%), op(1%), minor tm & sph, retro chl	fair fol(ms,qz), slight cren, qz augen, random bt, retrogression
K28d	qz(54%), ms(38%), gt(3%), bt(3%), op(2%), minor tm & sph	pronounced fol(ms,qz), layering(rel % ms,qz), poik gt - qz incl trails overgrow matrix fabric, bt overgrows fol, op parallel to fol, relict folding

K31a	qz(55%), ms(20%), bt(20%), chl(2%), op(10%), minor sph, tm & ap (op-gal,asp,sphl,ilm,po)	pronounced fol(ms,qz), slight cren, vague layering, op parallel to fol, bt overgrows fol
Calcareous Semipelites		
K18k	cb(40%), qz(30%), ms(20%), bt(7%), gt(<1%), op(2%), minor tm & sph, retro chl	variable degree of fol (ms), random bt with alt to chl, deformed clv in bt, late crenulation (S3)
K30c	qz(50%), ms(15%), cb(10%), bt(10%), pl(8%), Ksp(2%), op(<1%), minor sph & tm (op-a-r)	little fol, some flattening around qz augen
Psammites		
K14	qz(62%), ms(20%), pl(10%), Ksp(5%), gt(1%), op(1%), minor sph, ap & tm, retro sr	schistose fol(ms), qz & fsp augen show rotation, sr alt of fsp, bt and gt show retrogression
K15	qz(65%), ms(20%), bt(10%), pl(5%), op(1%), minor ap & sph, retro sr & chl	schistose fol(ms,bt), qz & fsp augen, alt to sr variable, chl after bt, lenses of pelitic material
K21d	qz(69%), ms(15%), bt(5%), gt(5%), op(3%), chlt(2%), minor ap, sph & tm, retro chl	schistose fol(ms,bt), qz augen with tails of qz & ms, xeno gt - qz incl trails are continuous with matrix, chl after bt, op largely parallel to schistosity
Pillow Lavas		
K49a	hb(65%), pl+qz(25%), chl(5%), ep(4%), op(<1%)	fine grained, no fol, folded qz/cb veins, yellow - green hb
50d	hb(60%), pl+qz(25%) chl(10%), ep(4%), op(<1%)	no fol, feathery chl, yellow - green hb
Metabasite (Dauphinee Brook)		
K16	hb(65%), pl+qz(23%), cb(10%), op(3%), minor chl	locally vague alignment, hb generally aligned, irregular patches of cb, weak cren (S2)

Amphibolite layers

K37a	hb(55%), pl(20%), qz(12%), op(10%), ep(3%)	no orientation of grains, idio to subidio hb, qz & pl are very strained
K38a	hb(40%), pl+qz(33%), op(13%), bt(7%), ep(7%)	generally random orientation, very strained qz & pl, planar fabric between random zones
K39a	hb(30%), pl(34%), qz(10%), op(13%), bt(7%), ep(5%), cb(<1%), retro chl & sr	fair fol(hb,bt),laths of hb intergrown with op, chl after bt, sr after pl, augen of pl

Schistose layers and shear zones

K36a	qz(70%), chl(10%), hb(2%), ep(5%), cb(3%), op(10%), minor sph (op-po,sphl,chal,gal,ilm, asp,hem)	patches of chl after hb, weak fol, late kinks (S3) in chl, op kinked with chl, hem alteration of po
K38e	hb(65%), qz(10%), chl(8%), cb(10%), ep(7%)	fine grained, intense fol due to shearing, isoclina folds in veins, late idio hb overgrows fol
K39b	qz&pl(40%), chl(25%), hb(25%), op(10%), minor ep & cb, (op-gal,asp,ilm, sphl,po,+/-py)	fair fol(hb,chl,qz), idio to xeno hb with qz incl, hb overgrows the fol, op parallel to fol, chl laths show kinking
K39c	op(60%), qz(30%), chl(10%), minor ep (op-asp,sphl,chal,+/-pyrl and man)	C & S planes in chl, late kinks (S3), undulose ext in qz, alteration of a Mn oxide or hydroxide

Felsic volcanic

K18	qz(30%), gt(25%), op(15%), ms(15%), bt(5%), chl(10%), (op-sphl,gal,asp,chal)	relict fol(ms,bt), layers of gt,op&qz, gt-incl trails(qz,ms) curved, retrogression of gt&bt to chl, polygonal qz
K21e	qz(60%), sr(30%), bt(5%), op(5%)	pronounced fol(sr,bt), qz augen with resorption texture and terminations, op parallel to fol

K21ee	op(50%), qz(34%), ms(16%), (op-asp,py)	layering(ms,qz), fol in ms layers, op finer in ms layers and coarse in qz layers
K28	op(40%), qz(35%), gt(10%), ms(15%), (op-gal,sphl,)	weak fol(ms), gt growing on op, polygonal qz, ms in patches
K28c	qz(48%), sr(41%), gt(10%), ms(<1%), op(<1%)	pronounced fol(qz,sr), poik gt - with curved incl trails(qz), large laths of ms assoc with the gt, gt growth during flattening

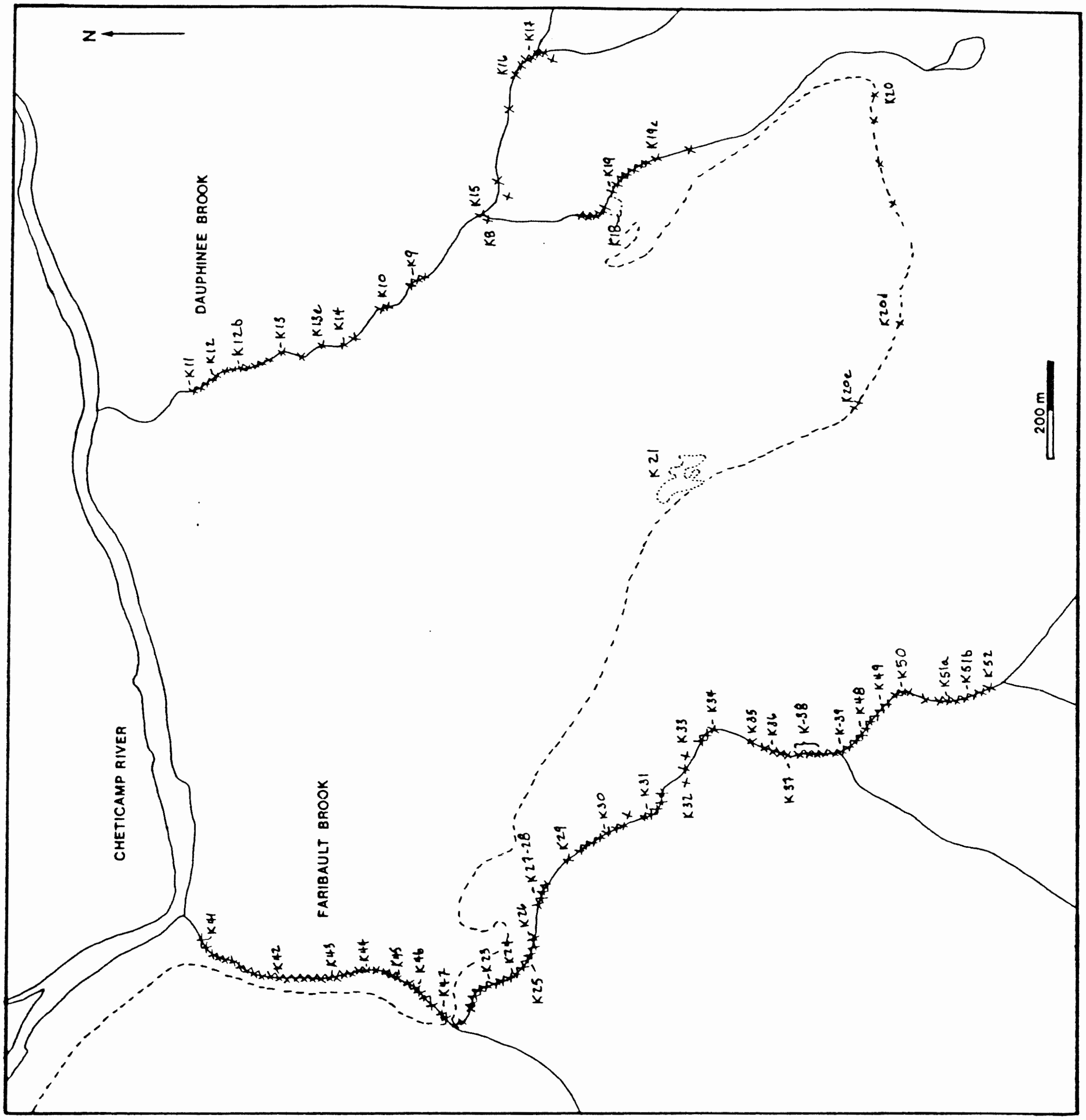

Figure A.1 Map showing location of samples.

APPENDIX B

The pillow basalt samples were analysed for ten major and minor oxides and fourteen trace elements on a Philips PW1400 sequential x-ray fluorescence spectrometer using a Rh-anode x-ray tube. Analytical precision is typically 5% or better for major and minor element oxides and 5-10% for trace elements. This is determined on replicate analysis. The samples were heated for 1 hour and 30 minutes at 1050 °C in an electric furnace to determine loss on ignition (LOI).

The samples were originally separated into groups depending upon which section of the pillow structure the samples represented. The ordering of the samples in the appendix is a result of this grouping. However, no obvious differences were observed between the groups.

APPENDIX B

Geochemistry of the Pillow Lavas

	40a	40b	49c	51b	40d	48b	48d
SiO2	46.38	48.09	45.90	45.71	48.25	46.05	48.40
AL2O3	14.89	15.01	15.41	15.95	14.80	14.76	14.56
FeO	10.52	9.58	9.76	10.81	9.34	10.17	10.99
MgO	10.59	9.85	9.16	9.73	9.56	8.73	8.74
CaO	10.29	9.60	10.82	10.75	10.32	11.43	8.37
Na2O	2.03	2.95	2.76	2.29	2.53	2.12	0.59
K2O	0.13	0.12	0.13	0.18	0.16	0.13	0.05
TiO2	0.78	0.72	0.85	1.03	0.80	0.99	0.91
MnO	0.18	0.17	0.14	0.20	0.17	0.20	0.22
P2O5	0.06	0.06	0.08	0.08	0.06	0.09	0.07
LOI	3.37	2.97	5.99	3.40	2.94	5.43	8.07
TOTAL	99.22	99.14	101.00	100.13	98.93	100.10	100.97
Ba	-	8	-	-	-	-	-
Rb	-	-	-	-	-	-	-
Sr	91	90	102	107	93	95	114
Y	24	22	26	29	23	28	26
Zr	45	41	49	57	47	59	50
Nb	3	3	4	3	3	4	3
Th	-	-	-	-	-	-	-
Pb	8	5	10	10	5	10	13
Ga	13	11	13	15	11	14	13
Zn	162	161	101	105	85	88	172
Cu	23	22	120	61	88	64	52
Ni	162	142	147	163	164	115	151
V	281	256	210	293	275	248	236
Cr	641	622	415	507	589	257	458
CIPW Norm Values							
Q	-	-	-	-	-	-	6.69
OR	0.80	0.74	0.81	1.10	0.99	0.81	0.32
AB	17.92	25.96	20.72	19.11	22.30	18.95	5.37
AN	32.48	28.46	30.81	33.82	29.75	32.09	39.76
NE	-	-	2.09	0.50	-	-	-
DI	16.65	16.89	20.59	17.04	18.94	22.33	3.66
HY	8.61	4.11	-	-	9.94	5.10	42.17
OL	21.84	22.28	23.09	26.22	16.36	18.52	-
IL	1.55	1.42	1.70	2.02	1.58	1.99	1.86
AP	0.15	0.14	0.20	0.19	0.14	0.22	0.17
TOTAL	100.00	100.00	100.00	100.00	100.00	100.00	100.00

APPENDIX B

Geochemistry of the Pillow Lavas

	49d	50d	40e	49b	50a	50b	50b3
SiO2	49.58	46.47	48.59	49.33	45.90	46.77	47.50
Al2O3	15.33	15.28	15.31	15.12	14.57	13.47	13.80
FeO	9.22	10.46	9.09	10.04	9.63	9.00	9.25
MgO	8.13	10.41	9.08	8.76	10.45	8.76	9.16
CaO	9.56	9.31	10.39	9.24	10.23	12.41	11.56
Na2O	3.13	2.66	2.66	3.02	2.67	2.69	2.96
K2O	0.22	0.18	0.15	0.16	0.22	0.25	0.25
TiO2	0.89	0.88	0.82	1.00	0.83	0.81	0.87
MnO	0.13	0.18	0.16	0.19	0.18	0.18	0.18
P2O5	0.07	0.07	0.06	0.07	0.07	0.07	0.07
LOI	3.03	4.17	2.71	2.72	5.17	5.50	4.23
TOTAL	99.29	100.07	99.02	99.65	99.92	99.91	99.83
Ba	-	-	-	-	8	13	7
Rb	-	-	-	-	5	4	5
Sr	103	93	105	101	96	86	90
Y	28	25	26	27	24	24	24
Zr	51	49	47	55	48	47	49
Nb	3	4	4	3	2	3	3
Th	-	-	-	-	-	-	-
Pb	15	10	7	8	16	12	18
Ga	12	11	15	18	11	15	14
Zn	127	113	113	117	107	85	85
Cu	15	98	93	98	66	110	101
Ni	140	183	165	158	177	129	141
V	261	285	281	284	251	247	258
Cr	419	591	624	466	588	443	482
CIPW Norm Values							
Q	-	-	-	-	-	-	-
OR	1.35	1.11	0.92	0.98	1.37	1.57	0.86
AB	27.51	23.47	23.37	26.36	20.91	18.84	21.40
AN	28.19	30.47	30.52	28.09	28.63	25.36	24.72
NE	-	-	-	-	1.59	2.85	2.60
DI	16.91	14.07	18.47	15.37	19.94	32.21	28.45
HY	10.67	1.79	9.50	11.86	-	-	-
OL	13.45	27.18	15.46	15.21	25.72	17.37	19.39
IL	1.76	1.74	1.62	1.96	1.66	1.63	1.73
AP	0.17	0.17	0.14	0.17	0.17	0.17	0.17
TOTAL	100.00	100.00	100.00	100.00	100.00	100.00	100.00

APPENDIX B

Geochemistry of the Pillow Lavas

	52a	49a	51a	48c	50c	40c
SiO2	46.40	50.11	48.67	51.56	46.59	43.84
Al2O3	15.91	14.25	15.94	14.38	16.70	15.88
FeO	10.54	7.36	9.35	8.59	10.05	11.39
MgO	11.23	6.32	7.57	7.87	9.10	10.55
CaO	8.60	12.81	10.02	9.40	10.06	11.02
Na2O	2.20	3.40	3.28	3.12	2.66	1.58
K2O	0.14	0.18	0.19	0.16	0.17	0.11
TiO2	1.09	0.72	0.89	0.73	0.93	0.88
MnO	0.19	0.15	0.18	0.18	0.18	0.18
P2O5	0.08	0.06	0.07	0.06	0.06	0.05
LOI	3.77	4.92	3.44	3.16	3.72	4.17
TOTAL	100.15	100.28	99.60	99.21	100.22	99.65
Ba	7	-	4	6	7	-
Rb	-	-	3	-	4	-
Sr	160	128	127	99	166	141
Y	25	22	25	22	26	25
Zr	59	45	51	45	52	49
Nb	3	3	3	3	4	3
Th	-	-	-	-	-	-
Pb	9	15	9	5	8	9
Ga	14	10	13	11	16	17
Zn	146	59	94	133	137	180
Cu	30	159	87	105	35	16
Ni	172	115	99	120	114	196
V	244	213	271	219	305	315
Cr	539	353	427	339	418	744
CIPW Norm Values						
Q	-	-	-	-	-	-
OR	0.86	1.12	1.17	0.99	1.04	0.68
AB	19.31	28.22	28.86	27.48	23.32	14.00
AN	34.37	24.21	29.34	25.78	34.33	37.61
NE	-	1.05	-	-	-	-
DI	7.63	34.39	18.01	18.34	13.93	15.82
HY	12.97	-	2.23	22.84	0.53	1.46
OL	22.52	9.38	18.48	2.98	24.87	28.55
IL	2.15	1.43	1.76	1.44	1.83	1.75
AP	0.19	0.19	0.17	0.14	0.14	0.12
TOTAL	100.00	100.00	100.00	100.00	100.00	100.00